Czech Technical University in Prague
Faculty of Electrical Engineering
Department of Control Engineering

OPTIMIZATION OF VENTILATION CONTROL IN THE BLANKA TUNNEL COMPLEX

Master's thesis

Vojtěch Talíř

Master programme: Cybernetics and Robotics
Branch of study: Systems and Control
Supervisor: Ing. Jan Šulc

Prague, May 2018

Thesis Supervisor:
Ing. Jan Šulc
Czech Technical University in Prague
Faculty of Electrical Engineering
Department of Control Engineering
Karlovo Náměstí 13
121 35, Prague 2
Czech Republic

Declaration

I hereby declare I have written this diploma thesis independently and quoted all the sources of information used in accordance with methodological instructions on ethical principles for writing an academic thesis. Moreover, I state that this thesis has neither been submitted nor accepted for any other degree.

In Prague, May 2018

.....
Vojtěch Talíř

ZADÁNÍ DIPLOMOVÉ PRÁCE

I. OSOBNÍ A STUDIJNÍ ÚDAJE

Příjmení: **Talíř** Jméno: **Vojtěch** Osobní číslo: **406299**

Fakulta/ústav: **Fakulta elektrotechnická**

Zadávající katedra/ústav: **Katedra řídicí techniky**

Studijní program: **Kybernetika a robotika**

Studijní obor: **Systémy a řízení**

II. ÚDAJE K DIPLOMOVÉ PRÁCI

Název diplomové práce:

Optimalizace řízení provozního větrání tunelového komplexu Blanka

Název diplomové práce anglicky:

Optimization of Ventilation Control in the Blanka Tunnel Complex

Pokyny pro vypracování:

1. Diskutujte jednotlivé možnosti řízení provozního větrání Tunelového komplexu Blanka (TKB).
2. Vytvořte linearizovaný matematický model proudění vzduchu TKB, porovnejte linearizovaný model se stávajícím nelineárním modelem a reálnými daty.
3. Na linearizovaném modelu navrhněte řízení provozního větrání pomocí matematického programování, které zajistí dodržení hygienických limitů koncentrací škodlivin uvnitř tunelu a zároveň dodrží požadavky na kvalitu vnějšího prostředí tunelu.
4. Výsledky regulace porovnejte pomocí simulace se stávající regulací, která pracuje s nelineárním modelem.
5. Vytvořte dynamický model šíření zplodin v TKB a porovnejte tento model se stávajícím statickým modelem a reálnými daty z TKB.

Seznam doporučené literatury:

[1] Šulc, J.: Řízení ventilace tunelu Blanka. Diplomová práce ČVUT FEL, květen 2012.
[2] Šulc,J ; Ferkl, L.; Cigler, J.; Zápařka, J. Model-Based Airflow Controller Design for Fire Ventilation in Road Tunnels. Tunnelling and Underground Space Technology. 2016, 60 121-134. ISSN 0886-7798.

Jméno a pracoviště vedoucí(ho) diplomové práce:

Ing. Jan Šulc, UCCEB Buštěhrad

Jméno a pracoviště druhé(ho) vedoucí(ho) nebo konzultanta(ky) diplomové práce:

Datum zadání diplomové práce: **15.01.2017** Termín odevzdání diplomové práce: **25.05.2018**

Platnost zadání diplomové práce: **30.09.2018**

Ing. Jan Šulc	prof. Ing. Michael Šebek, DrSc.	prof. Ing. Pavel Ripka, CSc.
podpis vedoucí(ho) práce	podpis vedoucí(ho) ústavu/katedry	podpis děkana(ky)

III. PŘEVZETÍ ZADÁNÍ

Diplomant bere na vědomí, že je povinen vypracovat diplomovou práci samostatně, bez cizí pomoci, s výjimkou poskytnutých konzultací. Seznam použité literatury, jiných pramenů a jmen konzultantů je třeba uvést v diplomové práci.

. Datum převzetí zadání

Podpis studenta

Acknowledgments

This diploma thesis would never be completed without huge support of many people and several institutions.

First, I would like to sincerely thank my thesis supervisor, Ing. Jan Šulc, for his patient guidance, encouragement and big support during my whole master studies. I also have to really thank my supervisor for advice he has provided throughout my Bachelor's and Master's degree as his student. I have been very lucky to have such a great guidance. My supervisor really cared about my diploma thesis and he has never rejected me with any question nor difficulties I faced along the fall of my studies. Jan Šulc has been very helpful with any issue I came with likewise open to all my suggestions and he responded to all my questions and queries so promptly.

Moreover, I would like to thank Feramat Cybernetics, spol. s r.o., not only for providing a place which allowed me to meet the supervisor, but also giving me the first opportunity to get in touch with real control design problem in industry and to cooperate on such amazing project like the Blanka tunnel complex truly is.

Completing this thesis would have been more difficult were it not for the support and friendship provided by my friends and members of the Czech Technical University in Prague and the Department of Control Engineering. A big thanks belongs to them as well.

Finally, I must thank my entire family and my girlfriend for enormous, continued support and encouragement during my whole studies at the CTU. In addition, I am also very grateful for all the prayers and love my closest have expressed for me.

Abstract

The master thesis is concerned with improvement, refinement and optimization of the ventilation operation in a tunnel having complex both a structure and ventilation system. This thesis can be divided into three main parts.

The first part deals with mathematical modeling of airflow dynamics in complex road tunnels. Namely, it focuses on derivation of a linearized mathematical model. The result of this part is a simplified simulation model of a tunnel containing mathematical model of airflow velocity based on Kirchhoff's laws for fluids dynamics, which includes all important factors influencing the airflow dynamics in a tunnel, i.e. piston effects of vehicles, air friction, effect of ventilation, etc.

The second part of the thesis presents how to derive concentrations model in a road tunnel. Two types of such model are introduced. The steady-state model of pollutant concentrations, which is the most used model in practice to describe behaviour of pollutants in road tunnels, is developed as well as a dynamic model of pollutant concentration, which stands on convection-diffusion equation.

The final part of the thesis suggests a possible improvement of the operational ventilation control of a tunnel based on mathematical optimization. The aim of these improvements is to reduce energy costs while keeping the control performance, since the ventilation in road tunnels forms a significant part of electricity costs. This objective is achieved by finding more convenient method how to solve an optimization problem.

The results of all parts of the thesis are validated on the Blanka tunnel complex in Prague, which is the largest city tunnel in Central Europe consisting of several entrance and exit ramps. Achieved results depict how to improve the control algorithm in the real operation. A comparison between couple of models of pollutant concentration and real measured data is shown as well as the linearized model of airflow velocity. The developed models, suggested improvements for the operational ventilation control and experimental validation using measured data are the main contribution of the thesis.

Keywords: Airflow velocity, Road tunnel, Optimization, Linearizion, Blanka tunnel complex, Pollution concentrations, Dynamic model.

Abstrakt

Diplomová práce se zabývá vylepšením a optimalizací provozního větrání v tunelu s komplexní strukturu i systém větrání. Práci lze rozdělit na tři hlavní části.

První část pojednává o matematickém modelování proudění vzduchu v silničních tunelech. Konkrétně se zaměřuje na odvození linearizovaného matematického modelu rychlosti proudění vzduchu. Výsledkem této části je zjednodušený simulační model tunelu, který obsahuje matematický model rychlosti proudění vzduchu založený na Kirchhoffových zákonech pro dynamiku tekutin. Tento model zahrnuje veškeré důležité faktory ovlivňující dynamiku proudění vzduchu v tunelu, jedná se o pístový efekt vozidel, tření vzduchu, vliv provozního větrání, a další.

V druhé části práce je vysvětleno, jak lze odvodit model koncentrací znečisťujících látek v silničním tunelu. Jsou představeny dva typy tohoto modelu. Model koncentrací v ustáleném stavu, který je v praxi nejpoužívanějším modelem pro popis šíření znečisťujících látek v silničních tunelech a dynamický model koncentrací znečisťujících látek, který je založený na difúzní rovnici.

Závěrečná část práce navrhuje možná zlepšení řízení provozního větrání v tunelu na základě matematické optimalizace. Cílem těchto zlepšení je snížit spotřebu energie při zachování stejných vlastností řídicího systému, protože provozní větrání v silničních tunelech představuje významnou část spotřeby elektrické energie tunelu. Tato část si klade za cíl najít vhodnější metodu pro řešení matematické optimalizace.

Výsledky všech částí diplomové práce jsou ověřeny reálnými daty z největšího městského tunelu ve střední Evropě, kterým je tunelový komplex Blanka v Praze. Výsledky popisují, jak vylepšit řídící algoritmus v reálném provozu. Navíc, hodnoty vypočtené modelem koncentrací znečišťujících látek i hodnoty dané linearizovaným modelem rychlosti proudění vzduchu jsou porovnány s reálnými naměřenými hodnotami z tunelovém komplexu Blanka. Hlavní přínos diplomové práce je implementace zmíněných modelů, navržené vylepšení řízení provozního větrání tunelu a ověření dosažených výsledků využívající naměřená data.

Keywords: Rychlost proudění vzduchu, Silniční tunel, Optimalizace, Linearizace, Tunelový komplex Blanka, Koncentrace škodlivin, Dynamický model.

Contents

Acknowledgements **v**

Abstract **vi**

1 Motivation **1**

1.1 Introduction 1

1.2 Case study 3

1.3 Organization of the Thesis 3

2 Optimal Control Strategy **5**

2.1 MPC control 5

2.2 Obstacles for Successful Implementation of MPC 8

2.3 Simplified Optimization-based Controller 9

3 Airflow velocity model **10**

3.1 State of the Art 10

3.1.1 Nonlinear airflow velocity model 11

3.1.2 Steady-state model of Airflow Velocity 17

3.1.3 Modification of Bernoulli and Continuity equation 17

3.1.4 Linearizion of the airflow velocity model 19

3.1.5 Results of linearizion 21

4 Emission model **25**

4.1 Introduction 25

4.2 Dynamic model 26

4.3 Steady-state model 28

4.4 Simulation results 30

5 Ventilation Control **33**

5.1 State of the Art 33

5.1.1 Possible control strategies of the operational ventilation control . . 34

5.2 Ventilation requirements 37
5.2.1 Normal ventilation 37
5.3 Operational ventilation in Blanka tunnel 38
5.3.1 State switch 39
5.4 Formulation of the optimization task 42
5.4.1 Feed-forward part 43
5.4.2 Decision variables 43
5.4.3 Cost function 44
5.4.4 Optimization task constraints 46
5.4.5 Feedback part 46
5.4.6 Solution of the optimization task 47
5.5 Finding a global solution 47
5.5.1 Simulation results 48

6 Conclusion **52**

A Appendix A **53**

1. Motivation

1.1 Introduction

We stand at the dawn of the fourth industrial revolution, an idea that will open new breakthroughs thanks to advancements in areas including artificial intelligence, robotics, advance control theory, quantum computing and the Internet of Things. An other technological growth area in recent years has been Big data. All sort of data are tracked, collected and analyzed. What is more, such data are also instantaneously logged and saved in data storages. Road tunnels are affected by this phenomena as well. However, the vast majority of road tunnels are equipped only by a minimum of data acquisition devices in past years, on the other hand, modern road tunnels are being equipped with sensor for measurement of physical quantities and this data are stored as well. Additionally, modern road tunnels regardless of theirs complexity, are equipped with latest technologies, infrastructure and expert systems. These up-to-date devices are put in place to ensure traffic safety in road tunnels so that the incidents can be prevented as far as possible and their impact can be kept to a minimum.

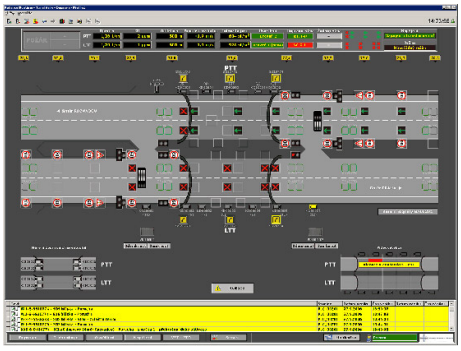

Figure 1.1: An example of HMI of a SCADA system of a road tunnel. [1]

Such an expert system which enables both data acquisition, visualization and control is a supervisory control and data acquisition (SCADA) system. SCADA is an automation control system widely used through numerous industry fields such as energy, oil and gas, electricity, traffic and many more. The SCADA system is emphasized, since several road tunnels complexes are controlled or monitored by such advanced monitoring system. In addition, the system provides numerous benefits such as redundancy adjustments, stable backups of time stamped data, secure alarm system, etc. It may also use scripts that detect problems in the system and quickly adjusts the plant from creating an outage. SCADA systems have the advantageous availability of cloud computing, therefore they

can report close to real-time accuracy and implement more complex algorithms. Otherwise, these algorithms would not be implementable on traditional PLCs.

On the other hand, despite many supervisory systems do acquire a big amount of operational data from a tunnel, these data are only logged and saved into convenient data storage without future usage. This kind of data containing numerous useful process variables of road tunnels would surely contribute to innovative developments in control strategy design point of view. Measured data could be than used to develop a model of process dynamics enabling to predict its future behaviour as well as to improve control algorithm. This derived model might form a vital part of advanced control design e.g., model predictive control having many advantages over the classical control strategies, where the model of process dynamics plays essential role.

Furthermore, the transport sector has become a major source of environmentally hazardous emissions [3] in recent years. Road tunnels have a significant importance in the transport infrastructure as they are located in valuables areas, for instance, cities, environmentally sensitive locations, etc. Especially in urban areas, they reduce impact on the surroundings in terms of air and noise pollution, where complex demands on the indoor IAQ and ambient environment of road tunnels are placed. On the other hand, they require extended design of tunnel technology, such as, traffic signs, ventilation and control systems. First, well-designed ventilation system and airflow velocity control can significantly improve conditions for evacuation, rescue and fire-fighting operations during fire. Second, during the standard operation of a tunnel, the efficient system of ventilation may significantly diminish electricity costs as well as improve quality of indoor environment and to ensure a protection of the ambient environment, as the operational ventilation of a road tunnel needs to keep pollutant concentrations inside the tunnel below defined limit values. All these directives emphasize crucial importance of ventilation control.

Figure 1.2: A schematic front view of a road tunnel with two lines. A jet fan can be seen on the right side of the tunnel tube. [2]

To summarize, the following objectives are important for successful operation ventilation control in road tunnels:

- maintenance of IAQ.
- protection of ambient environment,
- reduction of operational costs,

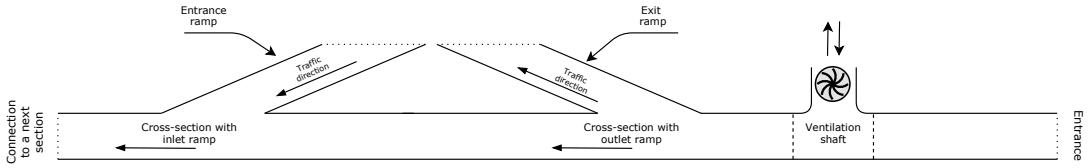

Figure 1.3: Schematic illustration of the tunnel cross-section with inlet ramp and outlet ramp U Vorlíku and a place for both airflow extraction and fresh air supply. Traffic direction is denoted by arrows.

1.2 Case study

The results are validated on the case study which is Prague's road tunnel Blanka. The Blanka tunnel is the largest city tunnel in central Europe consisting of complex geometry.

The Blanka tunnel complex in Prague forms the north-west part of the Prague City Ring Road. It is a tunnel complex meaning that, it consists of three road tunnels; Bubeneč, Dejvice and Brusnice, which are connected together through tunnel crossroads, say inlet or outlet ramps, as depicted in the Figure 1.3. It comprises a northern and southern tunnel tube supporting one-directional traffic. Besides the main two portals Malovanka and Trója, exit and entrance ramps are in each tube at two locations; Prašný Most and U Vorlíku. The tunnel crossroads U Vorlíku needs to be emphasized since measured data from the mentioned crossroad are used within the emission model involved in this thesis. The route pases urban development and partially also the historical center of Prague. The average traffic intensity is in the tunnel more than 70.000 vehicles per day.

For longitudinal airflow velocity control, a total of 88 jet fans is installed in both tubes enabling increase or decrease airflow velocity. In addition, the tunnel consist of three ventilation machine rooms (VMR) for the extraction of polluted air and control of fresh air supply, respectively.

Last but not least, data measured in the technology center of the tunnel are used within this thesis for comparison purposes and to create dynamic model of pollution in the program environment MATLAB [4].

1.3 Organization of the Thesis

The thesis is structured into 6 sections as follows: Section 2 states the goals which one would consider as the optimal control system of complex road tunnel. In 3, the derivation of the mathematical model of airflow velocity including its linearizion is presented. The dynamic model of pollutant concentration is introduced within the Section 4. This section provides a comparison of simulation and real measured data. The following Section 5 describes proposed improvement of current optimization-based control in the Blanka tunnel

Figure 1.4: Aerial map of the Blanka tunnel complex in Prague, Czech Republic. [JS]

complex. This section also contains a comparison of simulation data between the current and introduced approach. The thesis is concluded by Section 6 which summarizes the resulting observations.

2. Optimal Control Strategy

How the longitudinal airflow velocity should be controlled and which is the most suitable control algorithm? In road tunnels, usually several control techniques are used. Many of them are closed-lop with various logic elements [5] and some of them are feed-forward due to unreliable measurements of airflow velocity [6]. A recent published paper [7] introduces nonlinear feed-forward control with the feedback model linearizion. PI controllers are used for the vast majority of industrial processes.

Despite the PI controller has only two parameters for tuning, it is still difficult to find proper values of the proportional gain and the integral time constant. Improving classical control techniques as well as introducing advanced control strategies of operational ventilation control in road tunnels is desirable, because the standard control approach such as a rule-based or the PID control is not applicable in this situation, since it is a multiple input and multiple output (MIMO) system, which can not be easily decoupled. In addition, electricity costs reduction can not be achieved using aforementioned standard approaches, because they do not take any optimization into account. Minimizing a criterion, electricity costs in this case, can be accomplished only if the optimization-based control approach is used. Hence, the task is to suggest an advanced operational ventilation control in such complex tunnel taking some criteria into account, such as keeping the IAQ and minimizing operation costs.

2.1 MPC control

Furthermore, the object desired to be controlled with the MPC control strategy is an urban tunnel with several entrance and exit ramps. Usage of MPC might lead to optimize the operational ventilation control for given criteria. What is more, the pollution in the tunnel tube could be predicted according to appropriate model and measurements. Introducing predictive control approach may significantly reduce electric power consumption while keeping concentration of pollution within the required limits. The purpose of operational ventilation is to reduce the harmful gases with sufficient amount of fresh air.

The goal structure of the MPC for operational ventilation is illustrated in Figure 2.2.

Figure 2.1: On the left, the entrance ramp Prašný most can be seen. Additionally, a pair of jet fans is located at the ceiling of the tunnel.

It consists of the plant, i.e., a road tunnel with complex geometry, a predictive controller with feedback, an airflow velocity and concentrations sensors as well as its mathematical models, which generate predictions of controlled variables in order to estimate future behaviour of given system. Applying a such control scheme significantly increases ability to fulfill requirements on robustness and disturbance attenuation. In the depicted control scheme 2.2, the optimization block assembles the optimization task in order to minimize a cost function given as

$$J = \sum_{t=1}^{N} \left(y(t) - y_{\text{ref}}\right)^T \mathbf{Q} \left(y(t) - y_{\text{ref}}\right) + u^T(t)\mathbf{R}u(t) \tag{2.1}$$

subject to:

$$x_0 = \text{real measurement} \tag{2.2}$$

$$x(t+1) = \mathbf{A}x(t) + \mathbf{B}u(t) \tag{2.3}$$

$$y(t) = \mathbf{C}x(t) + \mathbf{D}u(t) \tag{2.4}$$

wherein $t = 1, ..., N$, where N denotes the length of receding horizon. The assembled optimization problem is also conditioned by physical constraints

$$u_{\text{LB}} \leq u(t) \leq u_{\text{UB}}. \tag{2.5}$$

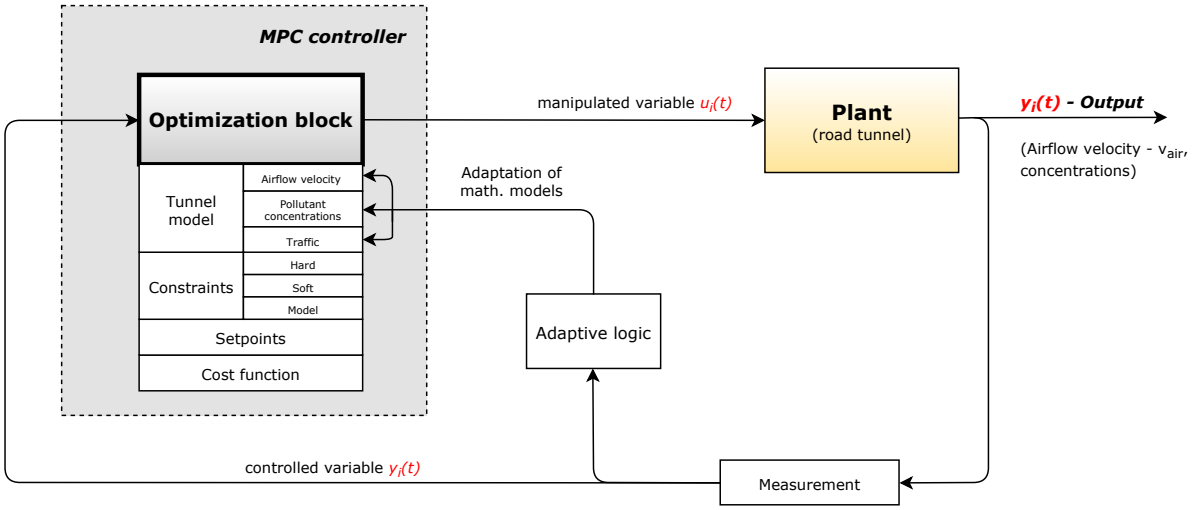

Figure 2.2: MPC controller block diagram.

The Model Predictive control (MPC) is a multi-variable control algorithm that minimizes a cost function J denoted by Eq. (2.1), an internal dynamic model of processes described by the Eq. (2.2) describing the plant and a history of past control inputs, to calculate the optimal control inputs. Cost function (2.1) is composed of weighting matrices $\mathbf{Q}$ and $\mathbf{R}$ penalizing deviation between measured manipulated variable $y(t)$ and a requested value y_{ref} likewise control inputs $u(t)$, respectively. In this case, inequality constraints are formed by soft-constraints and hard-constraints. The y_{ref} in cost function (2.1) forms the soft constraint representing desired airflow velocity defined by a setpoint. On the other hand, hard-constraints denote physical limitations of ventilation devices (jet fans and fans in ventilation machine rooms). They are expressed by Eq. (2.5), where the vector u_{LB} and u_{UB} mean lower and upper bounds on availability of ventilation devices. Equality constraints are represented by dynamic models of the plant described by Equations (2.2), where $x(t)$ is a vector of states i.e., airflow velocity and pollutant concentration at given time step, $u(t)$ denotes system inputs at specified time step consisting of a number of jet fans and fans in VMR to be switched on and traffic intensity.

Based on the optimization criteria, the predictive controller generates control signals $u(t)$ denoting the number of jet fans which are to be run. The control input is then passed to the plant acting on end devices. Additionally, the feedback is provided by the real measurement x_0 and ventilation devices. The MPC task is recalculated at each time step t. Typically for road tunnels, the sampling time of the MPC can be several minutes with respect to the slow process dynamics.

2.2 Obstacles for Successful Implementation of MPC

The future implementation of MPC supposes good knowledge of given system in order to create a model of particular behaviour. A linear models of road tunnels process are usually needed for MPC, since predictive control strategies are meant to be used. Such models that provide sufficient description of process dynamics are key base for the MPC control strategy. In order to control a process very accurately, a very precise model should be created. As [3] emphasize, "You can only control as precisely as you can model. Thus, if a highly tuned controller is desired, the very accurate model is needed." Nevertheless, it is important to stress out, that unfortunately the typical MPC algorithm requires knowledge of the process dynamic. The dynamic model of airflow velocity in the explicit form can be found for tunnels without ramps which are usually highway tunnels. Obtaining the dynamic model for complex road tunnels with connected ramps is challenging, as it is described in Section 2.2.

Implementation of typical MPC algorithm assumes simplified linear models which are not suitable for models of airflow dynamic in road tunnels. [8] Nevertheless, there are several obstacles that complicate achieving the goal state. The proposed airflow velocity model is not linear, thus its linearizion is inevitable. Additionally, the model of pollutant concentrations is described by a partial differential equation making difficult to use such model directly in the MPC controller. In order to implement models of pollutant concentrations in a road tunnel, its structure is appropriately divided into several sections. The pollutant concentration in the given section represents one system state. It is convenient to divide the entire tunnel into as many sections as possible in order to keep the accuracy of the model, however, by introducing new and new sections, the amount of system states gets higher. MPC could therefore have problems with computational time due to the tens of state variables and nonlinear process dynamics. For this reason, the number of section is needed to be set very carefully. Furthermore, knowledge of traffic distribution along the entire tunnel tube is required within the dynamic model of pollutant concentration, particularly, an accurate traffic model requires knowledge of exact position depending on time t of all vehicles in the tunnel. There are usually induction loops and traffic cameras to measure the total number of cars which have passed through the tunnel, thus an average value of vehicles passed through the tunnel is provided. What is more, the traffic information is delayed up to several minutes, because the measurement is evaluated after a certain time. For that reason, it is not possible to acquire exact information about traffic distribution along the whole tunnel.

2.3 Simplified Optimization-based Controller

Due to the aforementioned obstacles within implementation of the MPC controller in the Blanka tunnel complex, nowadays, the ventilation control system is a feed-forward controller with an adaptive logic. The feed-forward control is implemented via the static optimization. The feedback part is provided by the adaptive logic represented by the recursive least-squares algorithm with exponential forgetting. [8] It needs to be emphasized, that the current, say predictive, controller is not a classical linear controller in the usual sense. It is rather an optimization procedure that optimizes the trajectory of the output signal, while minimizing the energy consumption ensuring the physical or technological limitations of the system. A simplified steady-state model of airflow dynamics is used within the current control strategy of the Blanka tunnel complex shown in Figure 1.4. On the other hand, it has a few disadvantages though. First, optimization algorithm used in the feed-forward part is non-convex, hence the global minimum of resulted optimal control input is not ensured. Additionally, neither steady-state nor dynamic model of pollutant concentrations is incorporated into current optimization-based control.

Detailed description of the feed-forward controller with parameter feedback adjustment is provided in Section 5.4.

Thereafter, an attempt to improve the current optimization-based controller in the Blanka tunnel complex will be suggested within the thesis. The linearized model of airflow velocity is derived and validated on the Blanka tunnel complex. The linearized model causes that all constraints in the optimization task are convex. Second, the pollutant concentrations models are derived and validated in Section 4. These models can also be involved as constraints in the optimization task, and thus improve the overall control performance. The last improvement deals with finding of the global solution of the optimization task (5.1), which is described in Section 5.4. It concerns the comparison between local and global method and estimates energy savings that might be achieved.

3. Airflow velocity model

The chapter presents a detailed insight into modeling of airflow dynamics. The desired airflow controller performance is deeply influenced by the accuracy of the mathematical model. Hence, a significant effort is required to be put on the development of the airflow dynamics model. The non-linear mathematical model is based on the Bernoulli and Continuity equation. This non-linear model is than used to derive a linearized model of airflow velocity, which is suitable for the MPC control strategy and it is a crucial part of the operational ventilation control in any road tunnel.

The major contribution of this Chapter 3 is linearizion of the steady-state model of airflow velocity which is currently used within the optimization-based controller of operational ventilation (see Section 5.3) in the case study Blanka tunnel complex. Linearized model of process dynamics could be used in the design of a controller, which is based on quadratic programing (QP), and thus ensures the optimal solution of the optimization task 5.4.

3.1 State of the Art

In general, there are three possible approaches of airflow modeling in a road tunnel; Navier-Stokes equation, Euler equations and simplified one-dimensional models. The most general description of airflow dynamics in a road tunnel is provided by the Navier-Stokes equations. They are non-linear partial differential equations and are very accurate since the airflow dynamics can be modeled in three dimensions. The disadvantage is mainly theirs high demand on computational capacity, thus it is not convenient for the design of advanced airflow velocity controller, such as MPC. Next, the Euler equation can be obtained modifying the Navier-Stokes equations, particularly, by omitting terms which describe viscous actions. In addition, simplified one-dimensional models are given by Bernoulli equations and continuity equations. These simplified models are derived from Euler equations as well.

The simplified models of airflow dynamics in road tunnels require simplifying assumptions. The following key of them need to be emphasized. First, one-dimensional model

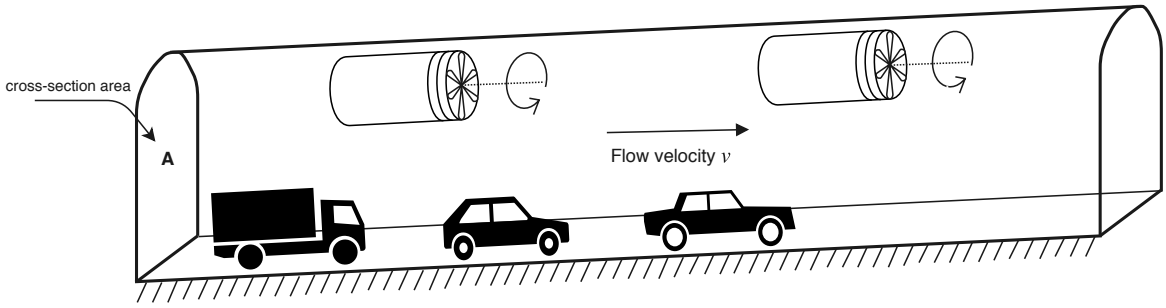

Figure 3.1: Longitudinally ventilated tunnel with no connected junction.

with lumped parameters is considered, i.e., $\frac{\partial v}{\partial y} = \frac{\partial v}{\partial z} = 0$ meaning the airflow velocity v does not depend on the y and z coordinate in a given section of the tunnel. This assumption significantly decreases computational demand. Second, the same direction of the traffic as the direction of the airflow velocity is denoted by a positive sign. Next, incompressible flow is considered, this means that the air density ρ is constant along the entire tunnel tube as well as it does not depend on time. This is valid for a road tunnels, where the average airflow velocity is about 7 m/s [9] These assumption simplifies complex models of process dynamics allowing design of classical controllers like PID as well as advanced controllers like MPC controller.

The road tunnel can be divided into several sections with set of parameters, such as cross-section area, airflow velocity etc. A schematic illustration of the tunnel section is depicted in Figure 3.1. The airflow velocity v is constant within the specified section. Additionally, each section contains generalized Bernoulli equation describing the airflow dynamics. Deriving of such simplified mathematical model of airflow velocity using the Continuity and Bernoulli equation is described further.

3.1.1 Nonlinear airflow velocity model

First, the simple case of a road tunnel without entrance nor outlet ramps and with unidirectional traffic is considered, as denoted in Figure 3.1. The Extended Bernoulli equation can be used to estimated airflow velocity in a road tunnel. As mentioned above, however the real liquid is compressible, the incompressible flow is consider in the thesis.

The Bernoulli equation for ideal liquid can be written for given two points in the tunnel tube as follows:

$$p_1 - p_2 + \frac{1}{2}\rho({v_1}^2 - {v_2}^2) = 0 \tag{3.1}$$

where p_1, p_2 [Pa] denotes the static pressure at two different points in the tunnel, ρ [kg m^{-3}] is the air density and v_1, v_2 [m s^{-1}] denote the airflow velocity at two given points of the tunnel.

For real flow and for a design of the operational ventilation controller, the Bernoulli equation has to be extended. Taking into account air friction, influence of other pressure changes and unsteady flow of air, the Eq. (3.1) is modified and it yields:

$$p_1 - p_2 + \frac{1}{2}\rho({v_1}^2 - {v_2}^2) - \rho \int_0^L \frac{\partial v(s,t)}{\partial t} \mathrm{d}s + \Delta p(t) = 0 \tag{3.2}$$

where L [m] is the length of the tunnel, $\rho \int_0^L \frac{\partial v}{\partial t} \mathrm{d}s$ represents the pressure change generated by unsteady flow and Δp [Pa] is the total pressure change in the tunnel caused by pressure losses and gains.

The airflow velocity is assumed to be constant along the entire tunnel section and does only depend on time. For this reason, a simplification is introduced as follows $v(s,t) = v(t)$, this means, $v_1 = v_2$. Additionally, the same atmospheric conditions such as, atmospheric pressure and temperature along the entire tunnel are considered and therefore the static pressure p_1 is equal to the pressure p_2, i.e., $p_1 = p_2$. Taking into account these assumptions the Eq. (3.2) is simplified to:

$$-\rho \int_0^{\mathrm{L}} \frac{\partial v(s,t)}{\partial t} \mathrm{d}s + \Delta p(t) = 0. \tag{3.3}$$

The Eq. (3.3) can be simplified even more since $v(t)$ is only a function of time. Solving the integral, the Eq. (3.3) is modified to:

$$-\rho \mathrm{L} \frac{\mathrm{d}v(t)}{\mathrm{d}t} + \Delta p(t) = 0. \tag{3.4}$$

The term $\frac{\mathrm{d}v(t)}{\mathrm{d}tt}$ can be rewritten as $a(t)$ and it is so called local acceleration. Thus, the final state of simplification of Extended Bernoulli equation is as follows:

$$-\rho \mathrm{L} a(t) + \Delta p(t) = 0. \tag{3.5}$$

The steady-state model of airflow dynamics can be used in case the rate of change of airflow is negligible compared to the sampling period of the model.

The total pressure change Δp is influenced by several factors in a road tunnel and they can be divided into minor and major losses. All pressure changes contributing to the mathematical model can be defined as follows:

$$\Delta p(t) = \Delta p_{\mathrm{fric}}(t) + \Delta p_{\mathrm{area}}(t) + \Delta p_{\mathrm{pist}}(t) + \Delta p_{\mathrm{jf}}(t) \tag{3.6}$$

where $\Delta p_{\mathrm{fric}}(t)$ [Pa] denotes the pressure loss given by air friction, $\Delta p_{\mathrm{area}}(t)$ [Pa] is local area loss, $\Delta p_{\mathrm{pist}}(t)$ [Pa], means influence of passing cars trough the tunnel tube, $\Delta p_{\mathrm{JF}}(t)$ [Pa] is the pressure change caused by running jet fans.

Air friction

The pressure loss caused by air friction mainly depends on wall roughness, placement of jet fans, sensors, etc. in tunnel tube, which forms an obstacle to the airflow. For that reason the pressure in a section is decreased. This pressure loss can be computed as follows:

$$\Delta p_{fric} = \frac{1}{2}\rho\lambda\frac{\mathrm{L}}{\mathrm{D_h}}v(t)\,|v(t)| \tag{3.7}$$

where L [m] denotes the length of given section of the tunnel, $\mathrm{D_h}$ [m] is hydraulic diameter of the tunnel and λ [–] is the dimensionless coefficient Darcy friction factor, which can be determined using the Swamme-Jain equation [10]

$$\lambda = \frac{1.318}{\left[\ln\left(\frac{\epsilon}{3.7\mathrm{D_h}} + \frac{5.74}{\mathrm{Re}(t)^{0.9}}\right)^2\right]}. \tag{3.8}$$

The term ϵ [m] is relative roughness. For simulation purposes the ϵ was set to $\epsilon = 0.015$ m. Re [-] is the Reynolds number. It is a similarity number denoting whether the airflow is laminar or turbulent. This coefficient depends on airflow velocity and viscosity as:

$$\mathrm{Re}(t) = \frac{|v(t)|\,\mathrm{D_h}}{\nu} \tag{3.9}$$

where the ν [$\mathrm{m^2\,s^{-1}}$] is the kinematic viscosity of air and it was set to $\nu = 15.07 \times 10^{-7}$. The non-linearity in the Eq. (3.9) can be omitted and thus the friction factor λ is considerable as constant value given as: $\lambda = 0.022$. [11]

Local area losses

The $\Delta p_{area}(t)$ represents the pressure loss due to local resistances such as, merging and dividing flows, cross-section area changes which depend on direction of airflow, shape of transition or cross-section area. Generally it is a quadratic function of airflow velocity and can be calculated as:

$$\Delta p_{area}(t) = -\frac{1}{2}\rho\zeta\,(v, \mathrm{A}, \mathrm{L}, ...)\,v^2 \tag{3.10}$$

where ζ [–] is the resistance factor depending on airflow velocity and tunnel geometry. Particularly, in case of a tunnel without connected ramps, this pressure loss can be rewritten providing detailed insight into terms which is composed of. Thus, it yields:

$$\Delta p_{area}(t) = \Delta p_{in}(t) + \Delta p_{out}(t) + \Delta p_{exp}(t) + \Delta p_{con}(t) \tag{3.11}$$

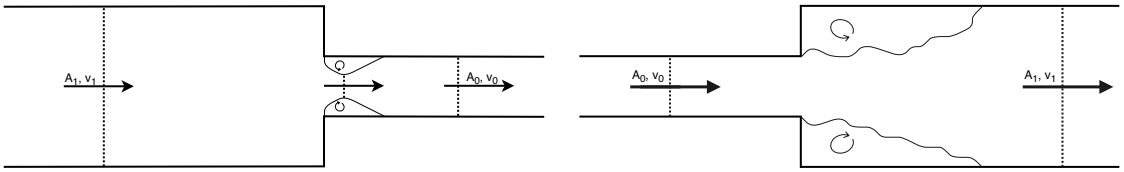

Figure 3.2: Sudden expansion an contraction of a tunnel section. Arrows denote direction of airflow.

where $\Delta p_{in}(t)$ [Pa] is the pressure loss at the entrance, however the $\Delta p_{out}(t)$ [Pa] denotes the pressure loss at the exit ot a tunnel tube, $\Delta p_{exp}(t)$ [Pa] is the loss generated by expansion of cross-section area and on the other hand the $\Delta p_{con}(t)$ [Pa] gives the pressure loss caused by contraction of tunnel tube.

The entrance pressure loss can be calculated as:

$$\Delta p_{in}(t) = -\frac{1}{2}\rho\zeta_{in}v(t)^2 \tag{3.12}$$

on the other hand, the exit pressure loss is given as follows:

$$\Delta p_{out}(t) = -\frac{1}{2}\rho\zeta_{out}v(t)^2 \tag{3.13}$$

where ζ_{in} [–] and ζ_{out} [–] are entrance and exit pressure loss coefficients, respectively. According to [12], these loss coefficients can be defined as $\zeta_{in} = 0.5$ and $\zeta_{out} = 1$.

Moreover, an another influence that causes a pressure loss is a change of cross-section area. Two types of shape transition are taken into account in the mathematical model of airflow dynamics. These are sudden contraction and sudden expansion, as depicted in Figure 3.2, since they are the most common changes in the shape of a road tunnel. The sudden contraction can be determined in the following way:

$$\Delta p_{con}(t) = -\frac{1}{2}\rho\zeta_{con}v_1(t)^2 = -\frac{1}{2}\rho\left(1 - \frac{\mathrm{A}_1}{\beta\mathrm{A}_0}\right)v_1(t)^2. \tag{3.14}$$

On the other hand, the sudden expansion can be calculated as:

$$\Delta p_{exp}(t) = -\frac{1}{2}\rho\zeta_{exp}v_0(t)^2 = -\frac{1}{2}\rho\left(1 - \frac{\mathrm{A}_0}{\mathrm{A}_1}\right)v_0(t)^2 \tag{3.15}$$

where $v_1(t)$ [$\mathrm{m\,s^{-1}}$] denotes the airflow velocity in the larger area, in comparison, $v_0(t)$ [$\mathrm{m\,s^{-1}}$] represents the airflow velocity in the smaller one, A_1 [m^2] denotes the larger area of the cross-section, however A_0 [m^2] corresponds to the smaller area of the cross-section and β [–] is the contraction coefficient, which can be determined in the following way:

[13]

$$\beta = 0.63 + 0.37 \cdot \left(\frac{\mathrm{A}_0}{\mathrm{A}_1}\right)^3. \tag{3.16}$$

The local area pressure losses are also caused due to merging or dividing flows in the tunnel tube, particularly in tunnel crossroads. These types of pressure losses are neglected in the mathematical model, because accuracy of the model is not significantly improved compared to computational demands of such pressure losses (Eq. 3.15 and Eq. 3.14).

Jet fans effect

The pressure gain generated by running jet fans depending on the airflow velocity and its angular velocity can be written as follows: [14]

$$\Delta p_{JF}(t) = \eta_{\mathrm{JF}} \rho v(t)^2 \frac{\mathrm{Q}_{\mathrm{JF}}(t)}{\mathrm{Q}(t)} n_{\mathrm{JF}}(t) \left(\frac{v_{\mathrm{JF}}(t)}{v(t)} - 1\right) \tag{3.17}$$

where $\mathrm{Q_{JF}(t)}$ [$\mathrm{m^3\,s^{-1}}$] is the airflow provided by the jet fan, $v_{\mathrm{JF}}(t)$ [$\mathrm{m\,s^{-1}}$] is the average output airflow velocity of a jet fan, $Q(t)$ [$\mathrm{m^3\,s^{-1}}$] is the airflow in the tunnel, η_{JF} [–] denotes the fan efficiency containing the correction of influence of the jet fans placement in the tunnel tube, $n_{\mathrm{JF}}(t)$ is the number denoting the amount of jet fans, which run simultaneously, $\mathrm{A_{JF}}$ [$\mathrm{m^2}$] is the outlet area of the jet fan.

Piston effect of vehicles

Passing cars through the tunnel tube increase the airflow. In case the velocity of vehicles is greater than airflow velocity, i.e. $u > v$, the term Δp_{pist} in the Eq. (3.6) is positive and denotes pressure gain. Conversely, if $u < v$ the piston effect causes a pressure loss. Additionally, the mathematical expression of piston effect also covers the situation when the direction of passing cars is opposite to the direction of the airflow. Thus, the pressure change caused by piston effect of passing vehicles can be expressed as follows:

$$\Delta p_{\mathrm{pist}} = \frac{\rho \sum_i \mathrm{N}_i(t) c_{d_i} \mathrm{A}_{v_i}}{2\mathrm{A}} \cdot (v_{\mathrm{car}}(t) - v(t)) \, |v_{\mathrm{car}}(t) - v(t)| \tag{3.18}$$

where c_{d_i} [–] is the drag coefficient of the respective type of vehicle, A_{v_i} [$\mathrm{m^2}$] is the frontal area of the passing vehicle, $v_{\mathrm{car}}(t)$ [$\mathrm{m\,s^{-1}}$] is the vehicle velocity in the tunnel and $\mathrm{N}_i(t)$ is the number of vehicles in the tunnel of the respective type.

The mathematical model differs three types of vehicles, which appears in a tunnel most frequently. These are passenger cars, vans and heavy cars. Values of frontal area as well as drag coefficients of selected vehicle type are presented in Table 3.1. Moreover, the

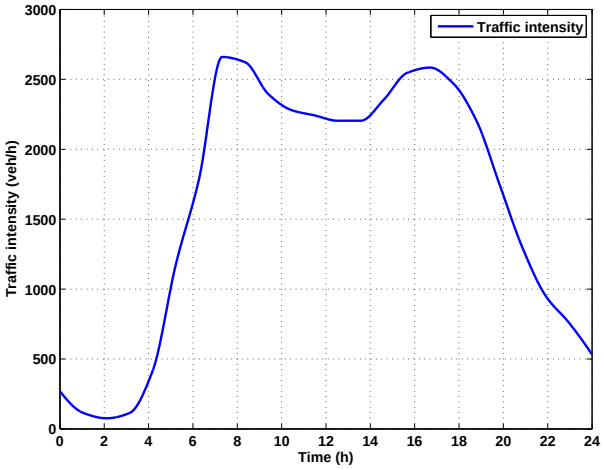

Figure 3.3: Representative values of hourly traffic intensity in the Strahov tunnel. [15]

Vehicle	**Drag coefficient** c_{d_i} [–]	**Frontal area** A_{v_i} [m^2]
Passenger cars	0.3-0.5	2-3
Vans	0.4-0.58	7-8.5
HGV	0.74-1.0	7-10

Table 3.1: Values of the frontal areas an drag coefficients of considered types of vehicles.

number of vehicles in a road tunnel section can be determined according to [11]

$$\mathrm{N_i}(t) = \frac{\mathrm{I}(t)\mathrm{L}}{v(t) \cdot 1000} \tag{3.19}$$

where $\mathrm{I}(t)$ [veh/h] is the hourly traffic intensity in given section and time, $v(t)$ denotes the velocity of vehicles and L [m] express the length of given section.

The hourly traffic intensity differs, yet has a specific progress during the day. Figure 3.3 depicts the typical hourly traffic intensity of passengers cars during the day in a tunnel.

Neglected pressure changes

First, the stack effect is generated due to differences in temperature at the entrance and exit tunnel portal. The air in a tunnel flows from the place with a higher temperature to the place with a lower temperature, since the natural buoyancy exists. The pressure loss due to stack effect is neglected in the mathematical model of airflow dynamics since the Blanka tunnel complex is located in urban area and also the altitude change between entrance and outlet portal is minor in comparison with piston or air friction pressure loss. Nevertheless, it can play a role of a disturbance effect. Second, similarly to the stack effect, the wind effect is very challenging to measure due to inaccuracy in wind speed and its direction measurement. Thus, the pressure changes caused by wind at the tunnel

portal are neglected, because of the suitable location in the terrain, especially in case of the Blanka tunnel complex, which is situated in urban area.

3.1.2 Steady-state model of Airflow Velocity

The mathematical model of airflow velocity is simplified for the design of the operational ventilation controller in the tunnel, because using the dynamic mathematical model of airflow velocity in order to design the controller is a difficult task, as the implementation of the dynamic model is challenging and the controller is expected to require high computational demands.

According to [16] the steady-state airflow dynamics can be considered during real operation, thus the following relationship is assumed

$$\frac{\mathrm{d}v_{\mathrm{air}}(t)}{\mathrm{d}t} \to 0 \tag{3.20}$$

meaning that, it is supposed that changes of airflow velocity during real operation are small enough compared to the controller step. Therefore, it is assumed that the airflow velocity is time variable, but steady state in each time. The static is given by set of non-linear algebraic equations as can be seen further in Section 3.1.3.

3.1.3 Modification of Bernoulli and Continuity equation

The mathematical model of airflow velocity may differ for tunnels consisting of several entrance and outlet ramps being ventilated longitudinally and for road tunnels which has no connected ramps and are equipped with airflow extraction system. Such tunnel complex can be divided into several sections, see Figure 3.4, intended to have constant geometry. In particular, a section is composed of following parameters: cross-section area, slope of the road, hydraulic diameter, number of traffic lanes, etc.

As depicted in Figure A.1 Blanka tunnel complex consists of several entrance and exit ramps, therefore the Bernoulli equations must be modified in order to fulfill pressure equality on connected ramps. The Bernoulli equations are used to fully describe the airflow dynamics in a road tunnel with connected ramps. As mentioned in Section 3.1.2,

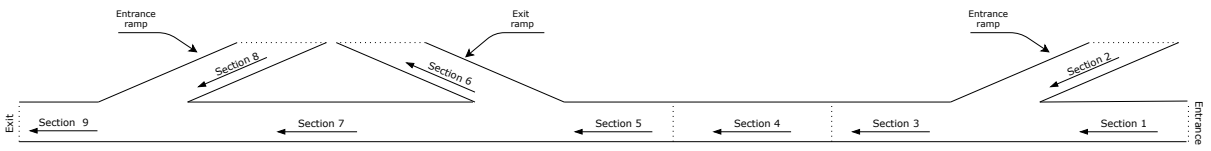

Figure 3.4: A schematic representation of a road tunnel complex containing ramps. The tunnel is divided into several sections with the constant geometry.

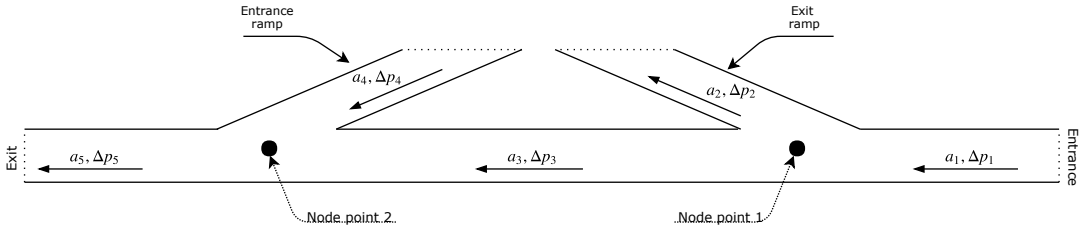

Figure 3.5: A tunnel complex containing connected entrance and exit ramp. Traffic direction is denoted by arrows.

the algebraic sum of pressure changes in a loop must be equal to zero: [17]

$$\sum_i \Delta p_i = 0 \tag{3.21}$$

where Δp_i [Pa] is the pressure change in the i-th section.

Eq. (3.21) represents the equivalent of the Kirchhoff's voltage law, where the pressure change is analogous to voltage. A tunnel crossroad depicted in Figure 3.5 can be described by the set of Bernoulli equations as follows:

$$0 = \Delta p_1 + \Delta p_2 \tag{3.22}$$

$$0 = \Delta p_2 - \Delta p_3 + \Delta p_4 \tag{3.23}$$

$$0 = \Delta p_4 + \Delta p_5 \tag{3.24}$$

where Δp_i denotes the total pressure change in the i-th section of the tunnel.

Moreover, if the constant airflow velocity along the entire tunnel section is assumed as well as the density of air, the continuity equation holds for the volumetric flow rates and for the non-stationary flows [17]. Therefore, these sections can be than mathematically connected via continuity equation, which is also called the mass-balance equation, and thus represents the conservation of mass:

$$\sum_i \mathbf{Q}_{v_i} = 0 \tag{3.25}$$

where $\mathbf{Q}_{v_i}$ $[\mathrm{m}^3\,\mathrm{s}^{-1}]$ is the volumetric flow rate in the given section of the funnel. The volumetric flow can be calculated as $\mathbf{Q}_{v_i} = \mathrm{A} \cdot v$.

The tunnel complex in Figure 3.5 can be described by two Continuity equations since there are two node points:

$$\mathbf{Q}_1 - \mathbf{Q}_2 - \mathbf{Q}_3 = 0 \tag{3.26}$$

$$\mathbf{Q}_3 + \mathbf{Q}_4 - \mathbf{Q}_5 = 0 \tag{3.27}$$

The continuity equations also hold for cross-section area changes and extraction as well as the supply of fresh air through the VMR.

3.1.4 Linearizion of the airflow velocity model

Although almost every physical system contains nonlinearities, usually its behavior within certain operating range of an equilibrium point can be approximated by a linear model with an uncertainty. The controlled system, in particular the model of airflow dynamics in a road tunnel is non-linear, however, a linear model of the plant might be required in the case of linear controller design. Linearizion of the steady-state airflow velocity model may significantly contribute to the design of linear controller or convex optimization task.

Furthermore, linearizion of the simplified mathematical model of airflow velocity being currently used in the case study Blanka tunnel complex, is introduced in this thesis.

The given non-linear Bernoulli equation (3.6), mentioned in Section 3, were simplified and replaced with a general linear equation having the following form

$$f(v) = \mathrm{a} \cdot v + \mathrm{b} \tag{3.28}$$

where $f(v)$ is a function denoting a pressure loss, a is a coefficient expressing the slope of linearized function and b is the intercept. Therefore, the following equation has to be found for the coefficients a and b

$$\Delta p_j = \mathrm{a} \cdot v + \mathrm{b} \tag{3.29}$$

where Δp_j is the corresponding pressure loss, a is the slope of the line and b denotes the intercept. Further, the slope of the line given by a can be determined as the derivative of δp_j evaluated at the specified point, i.e., the point of linearizion. Thus, the slope a can be calculated as follows:

$$\mathrm{a} = \left.\frac{\mathrm{d}\Delta p_j}{\mathrm{d}t}\right|_{v_0} \tag{3.30}$$

where the v_0 denotes the point of linearizion. Thus, the linear function can be written as

$$f(v) = \left.\frac{\mathrm{d}\Delta p_j}{\mathrm{d}t}\right|_{v_0} \cdot v + \mathrm{b}. \tag{3.31}$$

The coefficient denoting the intercept can be calculated from the equality of functions 3.28 and a non-linear Bernoulli equation expressing particular pressure loss Δp_j evaluated at the point of linearizion v_0. Thus, it can be stated as

$$\Delta p_j(v_0) = f(v_0). \tag{3.32}$$

Substituting (3.31) into (3.32) gives a formula for determining the intercept b of the linearized function as follows:

$$\mathrm{b} = \Delta p_j(v_0) - \left.\frac{\mathrm{d}\Delta p_j}{\mathrm{d}t}\right|_{v_0} \cdot v_0 \tag{3.33}$$

In addition, however the Bernoulli equation (3.6) is linearized, the continuity equation (3.25) is not, because they are already linear with respect to v_{air}.

Example: Linearizion of pressure loss due to friction effect

The above mentioned approach of linearizing Bernoulli equations is demonstrated on the following example. The linearized function denoting the pressure change due to friction effect is derived. Recall the formula expressing pressure loss due to friction effect given as:

$$\Delta p_{fric} = \frac{1}{2}\rho\lambda\frac{\mathrm{L}}{\mathrm{D_h}}v^2(t). \tag{3.34}$$

and a linear equation $f(v) = \mathrm{a} \cdot v + \mathrm{b}$ described by the slope a and the intercept b. The set of Eqs. (3.35) denotes how to calculate the a term from Eq. (3.28).

$$\begin{aligned} \mathrm{a} &= \left.\frac{\mathrm{d}\Delta p_j}{\mathrm{d}t}\right|_{v_0} && (3.35)\\ &= \left.\rho\lambda\frac{\mathrm{L}}{\mathrm{D_h}}v(t)\right|_{v_0} && (3.36)\\ &= \rho\lambda\frac{\mathrm{L}}{\mathrm{D_h}}v_0 && (3.37) \end{aligned}$$

where v_0 denotes the point of linearizion. The final formula expressing the term a is derived, thus $\mathrm{a} = \rho\lambda\frac{\mathrm{L}}{\mathrm{D_h}}v_0$. The intercept therm b can be determined form the equality given by the following equations:

$$\begin{aligned} \Delta p_{fric}(v_0) &= f(v_0) && (3.38)\\ &= \mathrm{a} \cdot v_0 + b && (3.39)\\ \frac{1}{2}\rho\lambda\frac{\mathrm{L}}{\mathrm{D_h}}v_0^2 &= \rho\lambda\frac{\mathrm{L}}{\mathrm{D_h}}v_0 + b && (3.40) \end{aligned}$$

thus, for the case of deriving linearized function of pressure change Δp_{fric}, caused by the friction effect, intercept coefficient b can be calculated as

$$\mathrm{b} = \frac{1}{2}\rho\lambda\frac{\mathrm{L}}{\mathrm{D_h}}v_0^2 - \rho\lambda\frac{\mathrm{L}}{\mathrm{D_h}}v_0. \tag{3.41}$$

Combining the Eq.(3.41) and the Eq. (3.35) yields:

$$f_{lin}(v) = \left(\rho\lambda\frac{\mathrm{L}}{\mathrm{D_h}}v_0\right)\cdot v + \left(\frac{1}{2}\rho\lambda\frac{\mathrm{L}}{\mathrm{D_h}}v_0^2 - \rho\lambda\frac{\mathrm{L}}{\mathrm{D_h}}v_0\right) \tag{3.42}$$

3.1.5 Results of linearizion

The result of system linearizion is provided in this Section. The simulation of the linearizion of the airflow velocity model proposed in Section 3 is performed for the Blanka tunnel complex. A comparison of the non-linear and linearized steady-state model with the real data is depicted in Figure 3.6 and 3.7 as well as in Figure 3.8. The steady-state airflow velocity model currently used in the Blanka tunnel complex is linearized. Additionally, the traffic intensity is also shown in these figures. The simulation is performed for one day of operation when the ventilation system is out of order, e.g. system maintenance, thus no additional flow is introduced by running jet fans, yet only natural ventilation occurs during a day. In this situation, traffic intensity is the only input to the mathematical model of airflow dynamics.

As can be observed, the linearized model provides satisfactory results compared to the

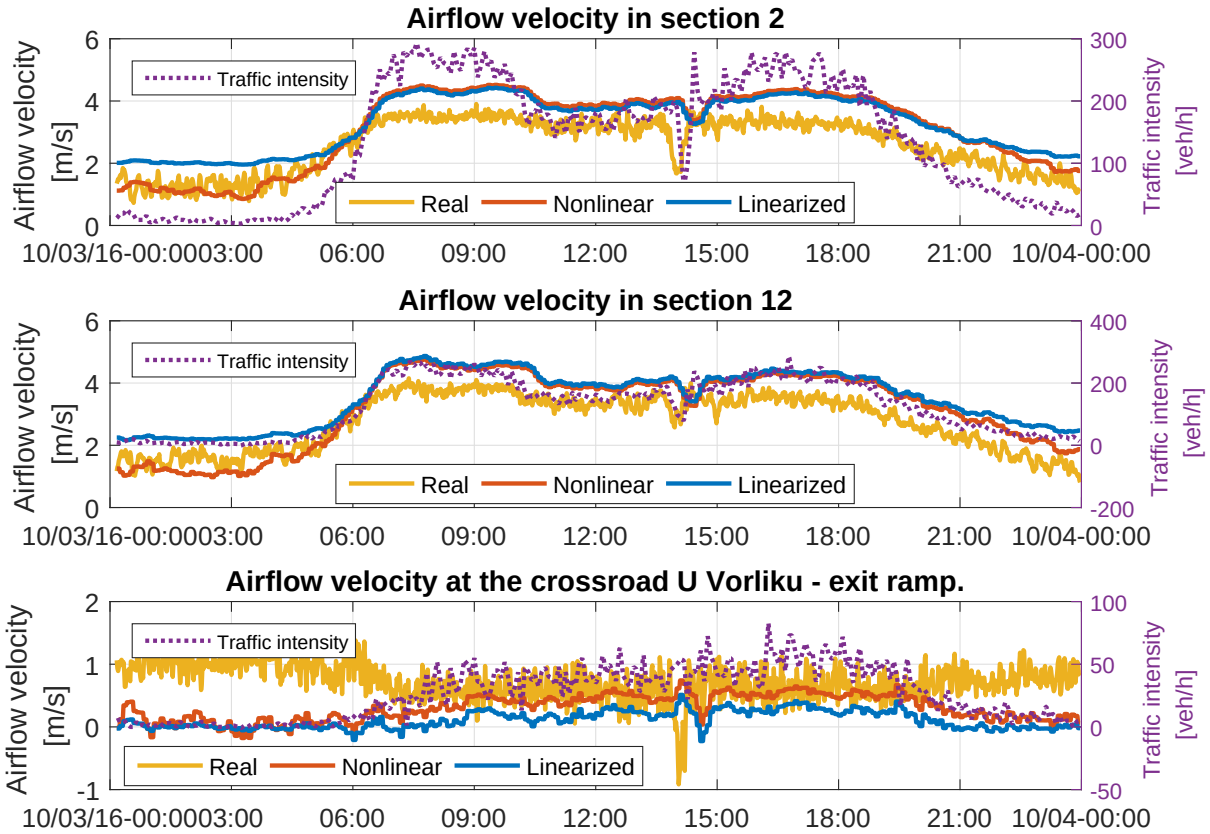

Figure 3.6: Northern tube of the Blanka tunnel complex. Outlet ramp U Vorlíků is emphasized. Presented section of the Blanka tunnel are shown in Figure A.2.

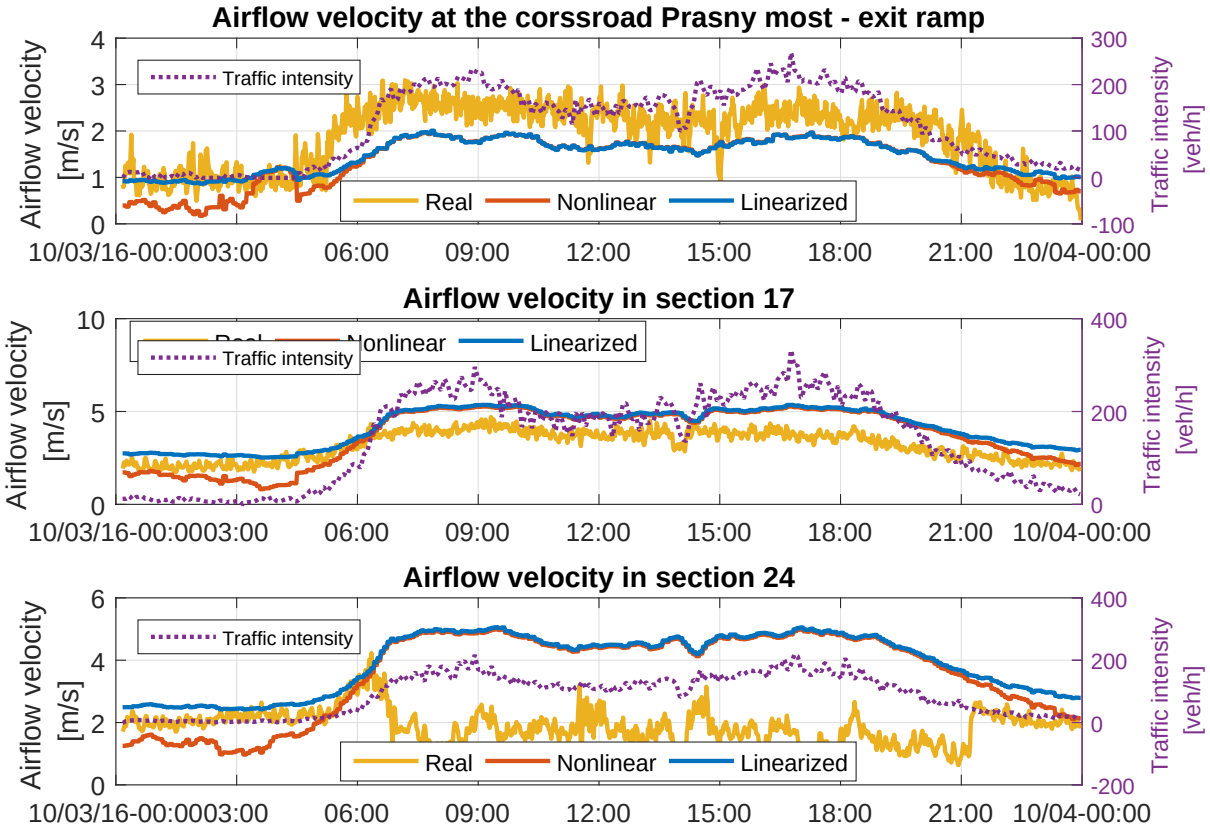

Figure 3.7: Northern tube of the Blanka tunnel complex with exit ramp Prašný most. Division of the Blanka tunnel complex into given sections can be seen in Figure A.2.

non-linear model and real measured data. Airflow velocity comparison in the north tunnel tube is shown in Figure 3.6 and in Figure 3.7, where the time progress of airflow velocity can be seen at the crossroads U Vorlíků and Prašný most as well as at several tunnel sections. On the other hand, obtained and measured airflow velocities in the southern tunnel tube of the Blanka tunnel complex are depicted in sub-figures 3.8a and 3.8b within

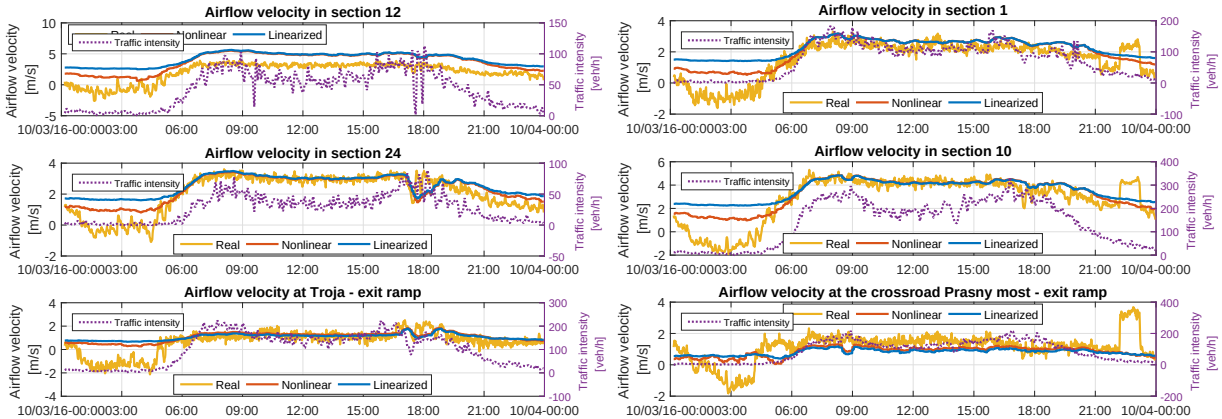

(a) Southern tube with Trója exit ramp.

(b) Southern tube with Prašný most crossroad.

Figure 3.8: The southern tube of Blanka tunnel complex. Figure A.2 denotes tunnel sections.

Table 3.2: Mean absolute errors of the linearized steady-state and non-linear steady-state model of airflow velocity for given section within the southern tube of the Blanka tunnel complex. Location of given section is visible in Figure A.2.

	MAE, m/s					
	Section 12	Section 24	Trója	Section 1	Section 10	Prašný most
Non-linear model	0.61	0.75	0.59	1.68	0.45	0.54
Linearized model	0.78	0.95	0.67	2.10	0.61	0.58

Figure 3.8.

As visible in all presented figures, values of airflow velocity obtained from the linearized model and these provided by the non-linear model differs till the 6:00 AM as well as from the 6:00 PM. However, at 6:30 AM the difference significantly decreases and these two quantities achieve practically the same values within 7:00 AM and 6:00 PM. This behaviour is expected and valid, since the linearized model can provide satisfactory results only in a sufficiently small neighborhood of the linearizion point.

Data from the month March 2016 are evaluated, and the simulation is performed within one entire day. The real measured data are denoted by the yellow line, however the linearized model and non-linear are represented by the blue and red line, respectively, and the violet dashed line shows the traffic intensity.

According to attached figures linearized model of airflow velocity provides valid results compared to the non-linear model. This fact is also confirmed in Table 3.3 and Table 3.2 wherein the mean absolute errors are denoted. The difference between the mean absolute error of non-linear model for depicted sections and the linearized model is not significant as one could expect, it is quite small instead. Therefore, based on the aforementioned results the linearized model of airflow velocity is suitable for the design of optimization-based control with linear equality constraints representing the linearized model.

To summarize, significant contribution of this Section 3 is linearizion of the already

Table 3.3: Mean absolute errors of the linearized steady-state and non-linear steady-state model of airflow velocity for given section within the northern tube of the Blanka tunnel complex.

	MAE, m/s					
	Section 2	Section 12	U Vorlíků	Prašný most	Section 17	Section 24
Non-linear model	0.66	0.59	0.47	0.57	0.92	2.03
Linearized model	0.71	0.76	0.63	0.51	0.98	2.05

developed airflow velocity model of the Blanka tunnel complex. The linearized model can be included in the design of a controller, particularly, within the optimization procedure. Having a linearized model of the process dynamics, quadratic programming can be applied to solve an optimization task, and thus improve the controller performance, likewise ensure minimal electricity consumption. Finding the optimal solution (global minimum) is guaranteed by the Quadratic programming that can be applied ones the linearized model is found. Unlike the currently used controller in the Blanka tunnel complex (see Section 5.3) does not ensure global minimum, solving the optimization task using Quadratic programming approach does guarantee the optimal solution.

4. Emission model

Dynamic model of pollutant concentration based on convection-diffusion equation is introduced in this section. The main contribution within this section is the implementation of this dynamic model of pollutants. Moreover, the stability of developed dynamic model is analyzed. Additionally, the steady-state model of pollutant concentrations in a road tunnel is derived. Finally, this section includes comparison of both models with against the real data from the Blanka tunnel. Simulations have been carried out for several working days of the week.

4.1 Introduction

The interest about air pollution has grown enormously in the last decades due to a better comprehension of the dangerous effects that some pollutants have on human health. A location where high concentrations can be expected are street canyon or road tunnels in which there are high emissions of pollutants in relatively small volumes. [18] High amount of venomous gases in a tunnel tube can be extremely dangerous for a human being. Additionally, the major responsible source of air pollution in urban ares is a vehicle traffic.

The combustion of fossil fuels by vehicles leads to road traffic emissions, which are significant sources of primary air pollutants. Road traffic emissions remain highly relevant as the most important emission source of air pollutant despite the successful implementation of catalytic converters in gasoline vehicles. [19] The emitted substances include several compounds, which are dangerous for human health.

However, carbon dioxide (CO2) is emitted in largest quantities contributing most to the anthropogenic radiative forcing, CO emissions per vehicle have reduced significantly due to usage of catalysts in vehicles. Thus, carbon monoxide is no longer key issue in ventilation design, however it is mainly focused on particulate matter and Nitrogen oxides, therefore measurements of only these gases is provided in the Blanka tunnel complex. Nitrogen dioxide and particulate matter are harmful for human health, moreover nitrogen oxides, NO_x : NO+NO_2, and carbon monoxide are secondary aerosols causing air pollutant

problems of photo smog in the outflow ot most large cities. The precise information of vehicle emissions passing through a road tunnel is crucial for the design of advanced operational ventilation controller as well as contribution of road traffic to environmental problems.

Emission factor (EF) which describes the emitted mass of a compound per driven distance are used to characterize traffic emissions. The EF depends on many variables such as size, type, fuel mode of the vehicle, road gradient and maintenance of the vehicle. Estimation of amount of air pollutant due to traffic is a difficult task, because of the diversity of above mentioned factors.

Therefore, modeling and calculation of air pollution due to traffic inside a road tunnel is challenging. This chapter gives overview how to model pollution concentration due to traffic inside a road tunnel, particularly, there exist two possibilities that describe the propagation of pollutants in the tunnel.

4.2 Dynamic model

Widely used dynamic model of pollutant concentration in road tunnels stands on the convention-diffusion equation [18]

$$\frac{\partial c(x,t)}{\partial t} + u_{\text{air}}(t)\frac{\partial x(x,t)}{\partial x} = D\frac{\partial^2 c(x,t)}{\partial x^2} + R(t) \tag{4.1}$$

where $c(x,t)$ [g/m^3] is pollution concentration, which depends of the position x and time t, $u_{\text{air}}(t)$ [m s^{-1}] is the airflow velocity in the tunnel, D denotes the diffusion coefficient [m^2 s^{-1}], $R(t)$ [gm/m^3/s] is the total amount of exhaust pollutants produced in specified section of the tunnel and it is a function of position and time because vehicles move in the tunnel and produce emissions in different locations and different times.

The pollutant production R mainly depends on so-called emission factor, number of the given type of vehicle, vehicle velocity and volume of air in the specified position in the tunnel tube [20]

$$R(t) = \frac{\sum_i N_i(t) E_i u_{\text{car}(t)}}{V_{\text{air}(t)}} \tag{4.2}$$

where u_{car} [m s^{-1}] denotes the velocity of passing cars, N_i [–] is the number of vehicles of the given type, E_i is the emission factor [g/m] and V_{air} [m^3] denotes the volume of air in the section and it is given as

$$V_{\text{air}} = \text{A}_\text{T} \cdot \text{L} \tag{4.3}$$

wherein the A_T stands for the cross-section are of tunnel tube at given position [m^2] and L

[m] is the length of the tunnel section. Production of vehicle emission highly depends on so-called emission factor E_i, which depends primary on the vehicle type (van, passenger car, truck, ...), slope of the road, etc. Tables containing these emission factors can be found in many sources depending on the European standards. The most used emission table for calculation of the emission factors in Europe is given by World Road Association (PIARC)[21], however other source is the program MEFA used for computational purposes of emission factors within the Czech Republic, which is developed by the company ATEM.

Values of longitudinal airflow velocities u_{air} in tunnel are usually within the $\pm 5\text{m}\,\text{s}^{-1}$. The value of the diffusion coefficient D can be estimated around 1×10^{-5} $[\text{m}^2\,\text{s}^{-1}]$ in gases, however the values vary for different chemical substances. Therefore, the fraction being multiplied by the D coefficient can be neglected in Eq. 4.1:

$$\frac{\partial c(x,t)}{\partial t} + u_{\text{air}}(t)\frac{\partial c(x,t)}{\partial x} = R(t). \tag{4.4}$$

The discretization of Equation (4.4) has to be performed in order to solve such equation. Nevertheless, the discretization is supposed to be accomplished in the way that Equation (4.4) is stable. It has to be emphasized, that the differential scheme varies for different airflow direction. Thus, in the case the airflow velocity is higher than zero, $u_{\text{air}} > 0$, the therm $\frac{\partial x(x,t)}{\partial t}$ is substituted by forward difference and the fraction $\frac{\partial x(x,t)}{\partial x}$ is substituted by backward difference, and on the other hand, by forward difference in the case of $u_{\text{air}} < 0$. Therefore, substituting these differences into Eq. 4.4, for the case when $u_{\text{air}} > 0$, yields

$$\frac{c_j^{t+1} - c_j^t}{\Delta T} + u_{\text{air}}^t \frac{c_j^t - c_{j-1}^t}{\Delta x} = R^t \tag{4.5}$$

and for the case when $u_{\text{air}} < 0$ it is modified as follows

$$\frac{c_j^{t+1} - c_j^t}{\Delta T} + u_{\text{air}}^t \frac{c_{j+1}^t - c_j^t}{\Delta x} = R^t. \tag{4.6}$$

Equation 4.5 is rearranged and the therm c_j^{t+1} is expressed in the following way

$$c_j^{t+1} = \left(1 - u_{\text{air}}^t \frac{\Delta T}{\Delta x}\right) c_j^t + u_{\text{air}}^t \frac{\Delta T}{\Delta x} c_{j-1}^t + R^t \Delta T, \quad u_{\text{air}}^t \geq 0, \tag{4.7}$$

and modifying Eq. 4.6 yields

$$c_j^{t+1} = \left(1 + u_{\text{air}}^t \frac{\Delta T}{\Delta x}\right) c_j^t - u_{\text{air}}^t \frac{\Delta T}{\Delta x} c_{j+1}^t + R^t \Delta T, \quad u_{\text{air}}^t \leq 0. \tag{4.8}$$

Stability of dynamic model

An important characteristic of a the dynamic model is stability. In order to provide valid outputs, the derived mathematical model of pollutant concentrations has to be stable. This is ensured if the values of the following two terms (4.9) and (4.10)

$$1 - u_{\text{air}}^{t} \frac{\Delta T}{\Delta x} \tag{4.9}$$

$$1 + u_{\text{air}}^{t} \frac{\Delta T}{\Delta x} \tag{4.10}$$

fall inside the unit circle, therefore the following inequalities must be fulfilled.

$$\left| 1 - u_{\text{air}}^{t} \frac{\Delta T}{\Delta x} \right| < 1, \quad u_{\text{air}}^{t} \geq 0 \tag{4.11}$$

$$\left| 1 + u_{\text{air}}^{t} \frac{\Delta T}{\Delta x} \right| < 1, \quad u_{\text{air}}^{t} \leq 0. \tag{4.12}$$

Rearranging Eqs. (4.11) and (4.12), the following inequalities are obtained denoting the stability condition for the dynamic model of pollutant concentration in a road tunnel

$$1 - \left| u_{\text{air}}^{t} \right| \frac{\Delta T}{\Delta x} \geq -1 \tag{4.13}$$

$$\left| u_{\text{air}}^{t} \right| \frac{\Delta T}{\Delta x} \leq 2. \tag{4.14}$$

The resulting inequality (4.14) expresses, how to properly choose the sampling time ΔT and the difference between each section Δx, where x denotes the distance inside the tunnel from the entrance. Values of parameters ΔT and Δx has to be chosen such that the inequality (4.14) is satisfied and also the computational demand is taken into account.

4.3 Steady-state model

The steady-state model can be used when changes in pollution concentrations are big enough compared to simulation step. Additionally, it does not require knowledge of traffic distribution along the entire tunnel tube, thus demands on model input are lower and more easy to accomplish compared to the dynamic model. Recall the simplified diffusion equation (4.4) which is the base for the steady state mathematical model of pollutant concentration as well. It is supposed that the system is time variable, however

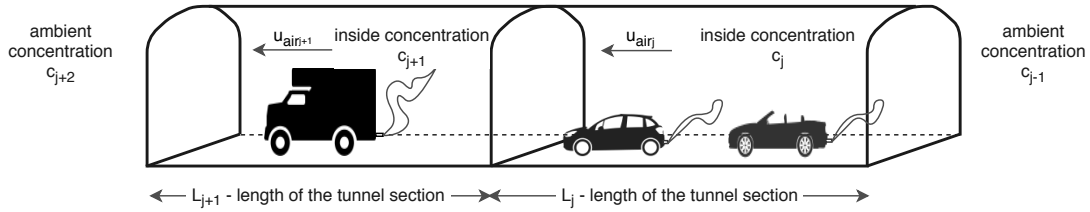

Figure 4.1: A graphical representation of pollutant concentration inside a tunnel containing several tunnel section.

steady state in each time, for this reason it is assumed that

$$\frac{\partial x(x,t)}{\partial t} \to 0; \tag{4.15}$$

meaning that changes in pollutant concentrations are fast enough under real operation compared to the sampling time of the simulation. Therefore, taking into account the previous assumptions, the partial differential equation (4.4) is modified to ordinary differential equation:

$$u_{\text{air}}(t)\frac{\mathrm{d}c(x,t)}{\mathrm{d}x} = R(t). \tag{4.16}$$

The equation (4.16) is substitutable as follows

$$u_{\text{air}}(t)\frac{c_j(t) - c_{j-1}(t)}{L} = R(t) \quad u_{\text{air}} \geq 0 \tag{4.17}$$

$$u_{\text{air}}(t)\frac{c_{j+1}(t) - c_j(t)}{L} = R(t) \quad u_{\text{air}} \leq 0. \tag{4.18}$$

where the situation from Figure 4.1 is considered. The pollutant concentration c_j is assumed inside the tunnel, which is the average along the tunnel section as well as the ambient pollutant concentration c_{j+2} and c_{j-1} at the tunnel portals. Therefore, concentration inside the tunnel at given section can be calculated as follows

$$c_j(t) = \frac{R(t)\mathrm{L}}{u_{\text{air}}(t)} + c_{j-1}(t) \quad u_{\text{air}}(t) > 0 \tag{4.19}$$

$$c_j(t) = -\frac{R(t)\mathrm{L}}{u_{\text{air}}(t)} + c_{j+1}(t) \quad u_{\text{air}}(t) < 0 \tag{4.20}$$

where the $c_j(t)$ denotes the pollutant concentration at $j-$th section, L is the length of the section, $R(t)$ represents produced pollutants by vehicles, $u_{\text{air}}(t)$ is the airflow velocity and $c_{j-1}(t)$, $c_{j+2}(t)$ denote the ambient concentration.

The steady-state model of pollution concentrations is time-dependent, yet steady-state in each moment in time. As expected, the result values are directly proportional to the length of the given section and produced pollutants by vehicles and at the same time

inversely proportional to the airflow velocity. It is key property within the tunneling experts. [20]

4.4 Simulation results

The results of both concentration models are presented on the case study, the Blanka tunnel complex. Resulted concentrations from the dynamic model are compared against measured data and concentrations provided by the steady-state model.

Simulation inputs are traffic data, which are measured in the Blanka tunnel complex. Emission factors used within the mathematical model of pollutant concentration depend on traffic distribution according to the European emission standard EURO. Furthermore, days 20. July 2016 to 25. July 2016 are chosen for simulation purposes. Within these days the pollutant concentrations were not influenced by the running ventilation, as the ventilation control system was under maintenance.

For the simulation purposes, the tunnel is divided into several sections with predefined length, slope, hydraulic diameter, etc. The length of shortest section is set to 100m and the time step is 10s. Thus $\Delta T = 10\text{s}$ and $\Delta x = 100\text{m}$. For this reason, the following inequality is raised

$$\left|u_{\text{air}}^{t}\right| \frac{\Delta T}{\Delta x} \leq 2 \tag{4.21}$$

$$5 \cdot \frac{\Delta T}{\Delta x} \leq 2 \tag{4.22}$$

and for $\Delta T = 10\text{s}$ and $\Delta x = 100\text{m}$, yields

$$0.5 \leq 2. \tag{4.23}$$

As can be seen from Eq. (4.23) the dynamic model is stable for chosen Δx and ΔT.

The following Figures 4.2 and 4.3 depict comparison of measured and obtained data in the tunnel section number 9 A.2. This specified section is chosen because measurement device of nitrogen oxides is present A.1, thus a valid comparison is provided. Additionally, the section 9 is located within the crossroad U Vorlíků, where the simulation was performed. Comparison of only NO_x concentration is provided, because concentration of carbon monoxide CO is not measured within the Blanka tunnel, since it is no longer the major source of exhaust pollutants due to development of vehicle engines. However, concentration of dangerous NO_x can overstep the limit values.

The Figure 4.2 as well as the Figure 4.3 depict the time progress of nitrogen oxides concentrations in the crossroad U Vorlíků, particularly in the section umber 9 A.2. The

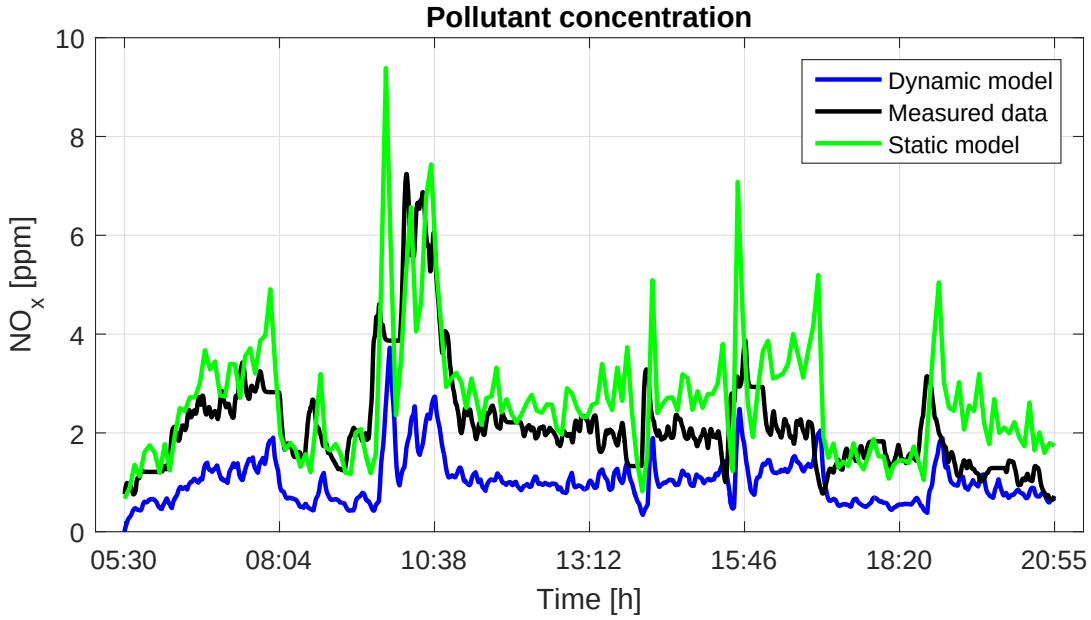

Figure 4.2: Simulation day 21. July 2016.

black curve represents measured concentrations by a nitrogen oxide sensor located in the section 9 A.2. The blue line depicts values of concentration provided by the dynamic model of pollutant concentrations and the resulted values of concentrations given by the steady state model are expressed by the green curve. It can be seen that both dynamic and steady-state mathematical model provide satisfactory results, however modeled data, especially results of the dynamic model shown in Figure 4.3a, differ a bit from measured values, yet in acceptable boundaries. It has to be stressed out that according attached Figures 4.2 and 4.3 the steady state model oscillates significantly compared to concentrations given by the dynamic model as can be seen mainly in the sub-figure 4.3a, 4.3c and 4.3d, however values of nitrogen oxides provided by the dynamic model acquire greater difference in value from measured concentrations compared to the steady state model.

If Figure 4.2 is inspected closer as well as Sub-figures 4.3b, 4.3c and 4.3d in Figure 4.3, one may observe there is almost constant difference between measured concentrations and values computed by the dynamic model. This situation can be clearly emphasized in Figure 4.2 from the 5:30AM to 10:00AM likewise from 10:38AM to 8:55PM, as well as in Figure 4.3b from 5:30AM to 6:00PM. Thus, it can be considered as an offset caused by setting initial concentration c^0_{amb} to zero during the simulation. Additionally, it can be noted that progress of pollutant concentration shown in Figure 4.3d is different compared to Figure 4.3a, 4.3b and 4.3c. This happens due to the contrast in traffic distribution, since the simulation day 4 4.3d is Sunday instead of a day within working week as it is in the case of the rest figures.

The implemented dynamic model of pollutant concentration is a white box model,

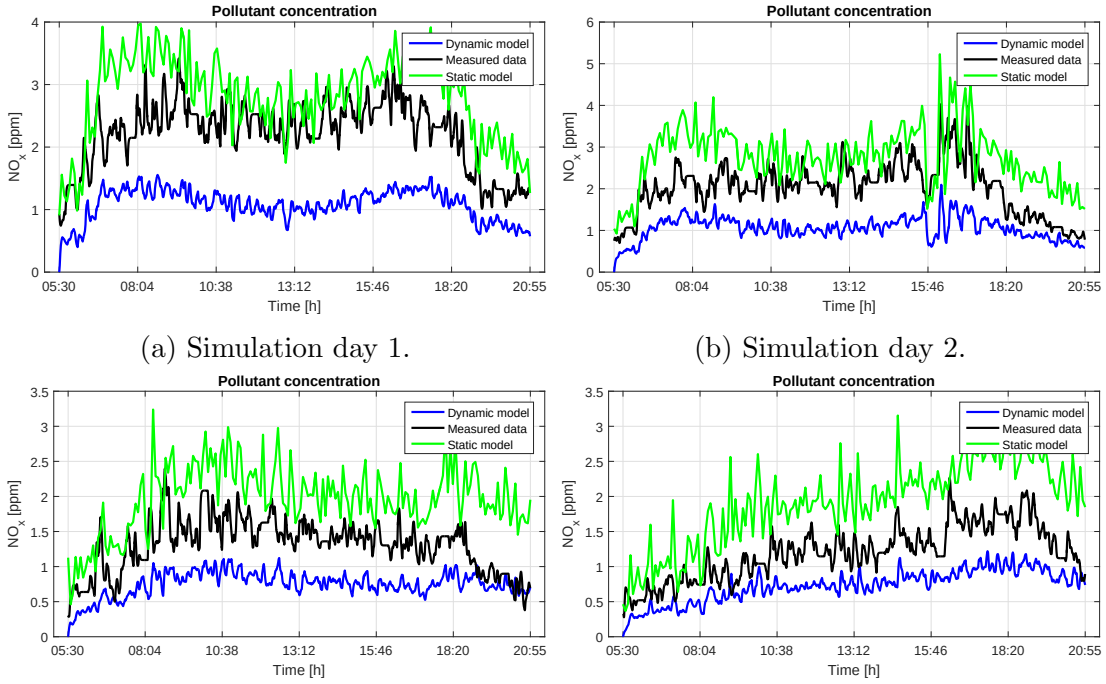

(a) Simulation day 1.

(b) Simulation day 2.

(c) Simulation day 3.

(d) Simulation day 4.

Figure 4.3: Simulation results provided by the mathematical model of pollutant concentration.

Table 4.1: Mean absolute errors of the dynamic and static model for given simulation days.

	MAE, ppm				
	Day 1	Day 2	Day 3	Day 4	Day 5
Dynamic model	1.15	1.18	0.98	0.57	0.47
Static model	0.63	0.76	0.78	0.66	0.71

because it is derived only based on physical processes in a road tunnel. No additional identification of process dynamics refining the mathematical model is introduced. Inaccuracy of dynamic model of pollutant concentration can be caused by several factors, such as the choice of the number of tunnel sections and theirs length as well as inaccuracies in distribution of both EURO categories and types of vehicles. In addition, mean absolute error (MAE) of resulting values estimated by both dynamic and static model of pollutants, respectively, is computed for each simulation day. MAEs are shown in Table 4.1. According to values of MAE in Table 4.1 both models provide resulting pollutant concentrations in allowable limits.

5. Ventilation Control

This chapter is focused on the operational ventilation control in roads tunnels. In this thesis the ventilation control is focused on complex road tunnels. As these types of tunnels occur usually in cities, there are often requirements on the quality of ambient environment, in order to minimize car exhaust fumes from exit junctions to nearby environment. Additionally, the operational ventilation should minimize electricity costs of ventilation devices, such as jet fans and fans in ventilation machine rooms.

This chapter's contribution is mainly in finding the appropriate method for the global solution of optimization task for the current ventilation controller in the Blanka tunnel complex, see Section 5.3. The algorithm is validated on the real data from the Blanka tunnel complex and the results are compared to the current optimization algorithm, which is the local one. The results of both algorithms (global and local) are compared in terms of energy costs and based on these results achieved energy savings by using the global method are estimated.

The first part of this chapter summarizes requirements and possibilities of ventilation control in road tunnels. The second part of this chapter provides an overview of current optimization-based controller in the Blanka tunnel complex. It also discusses the design of control structure and its components. The third part gives a proposal of convenient optimization algorithm solving the non-convex optimization tasks, which results in increasing energy cost savings of ventilation devices. The last part shows findings and results of the proposed global optimization approach.

5.1 State of the Art

There are still high demands on indoor air quality (IAQ), however the ventilation control is mainly designed for fire ventilation in road tunnels especially located in urban areas. Moreover, the operational ventilation is primarily focused on nitrogen oxides NO_x and PM because the combustion of engines and catalysts technology in vehicles have improved significantly during past years, and therefore CO is no longer the dominating factor for a design.[19]

Both objectives have the same principle; to handle the longitudinal airflow velocity.

5.1.1 Possible control strategies of the operational ventilation control

In recent years, there have been different control design techniques for operational ventilation control in road tunnels. These approaches can be separated into following areas:

- Rule-based control
- Fuzzy-logic control
- Optimization-based control
- MPC control

Rule-based control

The rule-based control strategy usually provides satisfactory results in case of road tunnels with no connected ramps and low demand on IAQ. Rule-based control strategies are easy to implement using the Programmable Logic Controllers (PLC), because there is not high demand on computational load, since the control algorithm contains only sets of conditions. Thus in this case, any additional computational devices, such as computational server, are not required compared to predictive control strategies. Additionally, rule-based control can not handle any optimization task, thus demands on minimizing energy costs can not be covered.

The rule-based control is strictly defined meaning that control actions are predefined according to a specific schedule. The time schedule is frequently used. Working days compared to weekdays require different ventilation program since the traffic distribution differs. Furthermore, hysteresis type of control is used in many cases. Typically, the rule-based control approach comprises both hysteresis control and time-scheduled ventilation control. For instance, a tunnel is ventilated naturally during night hours and predefined number of jet fans is running during scheduled time table, e.g. within the peak traffic hours for instance. And if the concentration of exhaust fumes reaches, say 70 %, of limit value, the number of running jet fans is increased until the measured pollutant concentration decreases below certain threshold.

Optimization-based control

Optimization-based control of operational ventilation is supposed to keep pollutant concentration under defined limit values. This control strategy also incorporates optimization

part of control algorithm so that minimizes a criterion. In vast majority of road tunnels the electricity costs of ventilation devices are minimized. Additionally, the advantage of this control approach is applicability to complex road tunnels with connected ramps and not only for highway tunnels as well as the ability to fulfill many requirements, such as air quality and to handle many constrained input variables, thus it is also applicable to MIMO systems. And thus, a model of process dynamics is required, particularly, model of airflow velocity, pollutant concentration and traffic model have to be usually introduced. In Ref. [22] dynamic model of airflow velocity and concentration was introduced. And for example as Ref. [23], [24] denotes, a quasi-dynamic model of airflow velocity based on Bernoulli and continuity equations is derived describing the behavior of process dynamics.

Optimization-based control design can not be considered as MPC control because process variables estimation is not used within the control algorithm.

Fuzzy-logic control

Other approaches have applied fuzzy logic control (FLC). During the past several years, fuzzy control has emerged as one of the most active areas for research in the applications of fuzzy set theory, especially in the field of industrial processes, which are challenging to control by conventional methods due to the lack of quantitative data regarding the input-output relations. [25]

The term fuzzy refers to the fact that the logic involved can deal with concepts that cannot be expressed as the 'true' or 'false' but rather 'partially true'. The fuzzy logic has the advantage that the solution a problem can be cast in terms that human operators can understand. [26]

This Fuzzy-logic control has some advantages over the traditional control systems, such as PID. In many cases the mathematical model of process does not exist, or it is too complex, or requires high demands on computational power and memory, therefore a system based on empirical rules might be more effective. Additionally, fuzzy control can be used to improve existing traditional system controller by adding an extra layer of intelligence to the current control method.

Karakas [27] presented a fuzzy-logic control design for the control of highway tunnel ventilation. The proposed control structure aims to maintain only a single process-state variable defined at a set point. The controller is a fuzzy logic controller, where its inputs are an

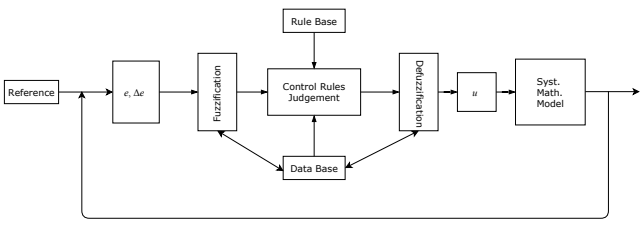

Figure 5.1: Schematic illustration of a fuzzy-logic controller. [27]

error end a change of error and the out-
put being the required change in the controlled variable. For demonstration purposes, the structure of mentioned controller is depicted in the Figure 5.1. There can be seen blocks representing both fuzzification and defuzzification process, a controlled plant given by a mathematical model and a module containing decision making components, such as judgment algorithm, a set of defined rules and data base enabling inputs and outputs to be fuzzificated and defuzzificated, respectively. According to the attached results, a comparison of power consumption of ventilation devices is denoted. Author shows that in the case where FLC control is applied the electric power consumption is 4,48 times lower compared to the situation where classical control approach is used. The control system was applied only on highway tunnel with no connected ramps and the possible extension for a tunnel having complex structure is not discussed either.

Bogdan et. all [28] described a model predictive and fuzzy control algorithm for a longitudinal ventilation system in a road tunnel. MPC controller is applied together with fuzzy logic controller as the additional control layer. Since the model of process dynamics in the tunnel describes real plant only to certain level, the fuzzy controller is integrated aiming to provide steady state accuracy. It compares the required level of pollutant with the measured value and adjust the jet fans prediction in order to keep the pollution close to the defined level. Simulation results of proposed scheme show that time response of the operational ventilation is much faster compared to the system controlled by conventional controller. Moreover, energy consumption is reduced around 5 % for simulated situation. The simulated behavior and expected ventilation system performance during real operation in the tunnel is also verified. Finally, it is shown that the proposed algorithm keeps concentration of pollutants within predefined limits.

MPC control

Predictive control seems to be a promising control approach that can help to improve properties of existing ventilation systems applied in many road tunnels. Model predictive control is a control method or group of control methods which make explicit use of a process model to obtain the control signal by minimizing an objective function. The main benefit of MPC is its constraint handling capacity and an ability to cover multiple-input and multiple-output system. Unlike most other control strategies, constraints on inputs and outputs can be incorporated into the MPC optimization.[29] Another advantage of MPC is its ability to handle future events as soon as they enter the prediction horizon. Basic control design approaches, typically a PID type of control law does not involve any future prediction. It deals with potential disturbance once it reaches it. On the other hand, the feed-forward part can be added but the design could be somewhat ad hoc. The

systematic feed-forward design is integrated with the constraint handling.

Even though the MPC has many important advantages mentioned above, implementing the MPC control strategy in road tunnels is still limited because of several difficulties. First, MPC algorithm is based on knowledge of process dynamics, thus it is required to obtain the dynamic model for complex road tunnels with connected ramps. This task is difficult, however the dynamic model in the explicit form can be derived for tunnels without connected ramps, such as high tunnels. Second, in case of the Blanka tunnel complex there is a lack of sensors, therefore many variables such as opacity or NO_x have to be estimated. Additionally, simplified dynamic models are assumed within typical MPC algorithm, unfortunately these models are unsatisfactory for modeling airflow dynamics in road tunnels.

Publication [30] and [31] provide simulation analyses of operational ventilation. Airflow dynamics in three-dimensions is created and simulated with derived predictive controller. As authors emphasize, presented results confirm higher effectiveness of predictive control approach, thus it is a perfect candidate to be used aiming to reduce effectively the values of pollution inside the road tunnel tube. Unfortunately, they do not present any experimental validation of designed predictive controller.

5.2 Ventilation requirements

There are two levels of ventilation in road tunnels, i.e. normal ventilation and fire ventilation. The fire ventilation is not covered in this thesis, however the ventilation under normal operation of road tunnel is discussed in the thesis.

5.2.1 Normal ventilation

The operational ventilation must ensure the desired quality of the indoor environment, i.e it has to maintain the concentration of pollutants within defined limits. The carbon monoxide, nitrogen oxides and opacity are usually considered as exhaust gases. Visibility is the inversion value of opacity and it holds that the better visibility is in the tunnel, the lower values of opacity are in the tunnel. There exist several organizations, such as PIARC [21] or CETU [32] acting among Europe publishing recommendations how to define limit values of pollutants concentration for respective type of a tunnel, because there are no strictly given directives defining such boundaries. Limit values of pollutants concentration used in road tunnel in the Czech Republic are denoted in the Table 5.1.

City tunnels are located in urban areas surrounded by the build up area, and thus there can occur additional requirements to ensure also protection of outdoor environment of the tunnel from pollutions of passed cars. The objective is to keep the polluted air

Pollutant	Limit value
carbon monoxide (CO)	70 ppm
nitrogen oxides (NO_x)	10 ppm
opacity	0.005 m^{-1}

Table 5.1: Limit values of pollutant concentrations.[21]

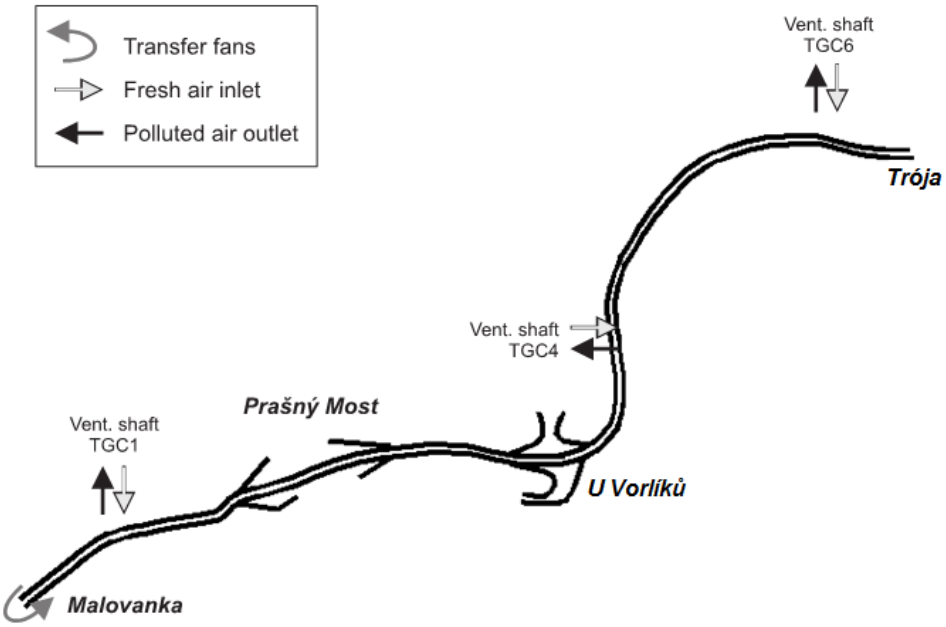

Figure 5.2: Schematic representation of ventilation machine rooms within Blanka tunnel complex. [15]

inside the tunnel to be withdrew by ventilation shaft instead of being moved outside of tunnel through exit ramps or main exit portal, because pollutants dissolve in the upper atmosphere. [20]

5.3 Operational ventilation in Blanka tunnel

Figure 5.2 depicts a schematic view of the operational ventilation in the Blanka tunnel. The tunnel is equipped with jet fans alongside both northern and southern tunnel tube as well as ventilation machine rooms shown in Figure 5.2. It can operate in five different states. The operational ventilation is activated as soon as the tunnel is not in a state of emergency, e.g. during a fire. The exact switching conditions and transients between states are described in the following Section 5.3.1.

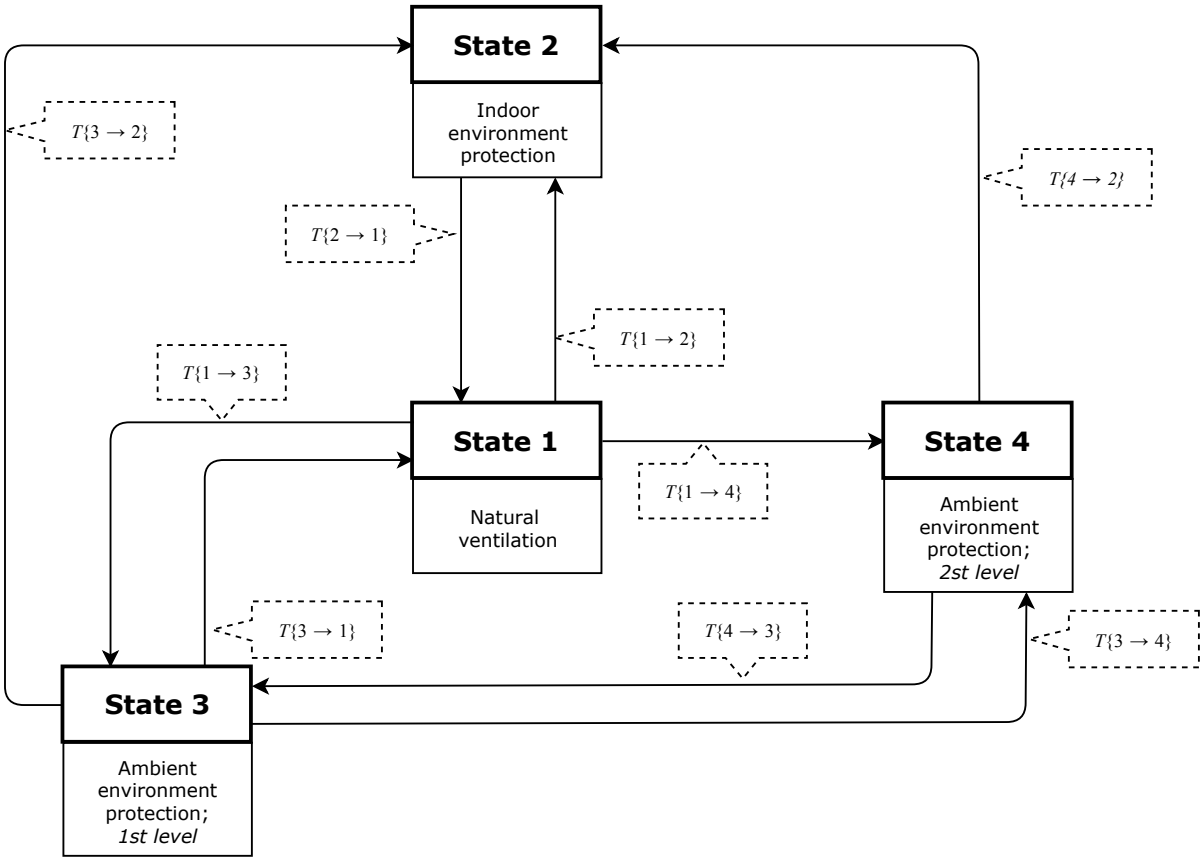

Figure 5.3: A state diagram of the state switch, which activates the required state of operational ventilation based on several conditions. The fifth mode (pre-ventilation) of operational ventilation is not depicted, because it is activated only in case of suspicion of fire.

5.3.1 State switch

The required state of operational ventilation is activated by the state switch and it can function in five states:

1. Natural ventilation.
2. Indoor environment quality control.
3. Protection of the ambient environment; first level.
4. Protection of the ambient environment; second level.
5. Pre-ventilation mode.

The state of operational ventilation is set based on the following parameters: traffic intensity in the northern tunnel upstream of the Malovanka portal (Figure A.2), inside NO_x concentration and opacity, current operating time and outside air velocity at the

Malovanka portal. Table 5.2 shows transient conditions between possible states of operational ventilation except the pre-ventilation mode, because it is activated only in case fire pre-alarm is detected.

Transition	Condition
T{1 → 3}	traffic intensity ≥ 1000 veh/h
T{1 → 2}	$c_{\text{meas}} \leq$ limit value
T{2 → 1}	$c_{\text{meas}} \leq 0.75 \cdot$ limit value
T{3 → 2}	$c_{\text{meas}} \geq$ limit value
T{4 → 2}	$c_{\text{meas}} \geq$ limit value
T{3 → 1}	traffic intensity ≥ 800 veh/h

Transition	Condition
T{3 → 4}	$v_{\text{out}} \geq 0.75\,\text{m}\,\text{s}^{-1}$ **and** traffic intensity ≤ 2250 veh/h
T{4 → 3}	$v_{\text{out}} \leq 0.5\,\text{m}\,\text{s}^{-1}$ **and** traffic intensity ≥ 1000 veh/h **or** traffic intensity ≥ 2250 veh/h
T{3 → 4}	$v_{\text{out}} \leq 0.5\,\text{m}\,\text{s}^{-1}$ **or** traffic intensity ≥ 2250 veh/h
T{1 → 4}	$v_{\text{out}} \leq 0.5\,\text{m}\,\text{s}^{-1}$ **and** traffic intensity ≥ 1000 veh/h **or** traffic intensity ≥ 2250 veh/h

Table 5.2: Transient conditions between given states of operational ventilation. c_{meas} represents the measured values of pollutants concentration and v_{out} is the airflow velocity at the Malovanka portal.

State 1: Natural ventilation

Within this state, the tunnel is ventilated naturally, longitudinally due to the piston effect of passing cars. Natural ventilation, State 1, is activated if and only if there is low traffic intensity in the tunnel, i.e. it does not exceed 1000 vehicles per hour and concentration of pollutants do not exceed limit values depicted in Table 5.1. Additionally, State 1 is implicitly applied during night hours, i.e. from 9:00 PM to 6:00 AM, to reduce noise produced by running fans. Moreover, there are no requirements for the IAQ and a protection of the ambient environment within this state.

State 2: Protection of the indoor environment

State 2, Protection of indoor environment is switched on if the limit values of pollutant concentrations are exceeded. The operational ventilation must ensure the enough supply

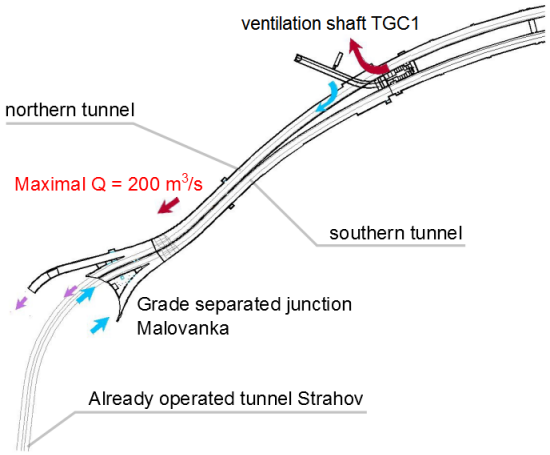

(a) First level of protection.

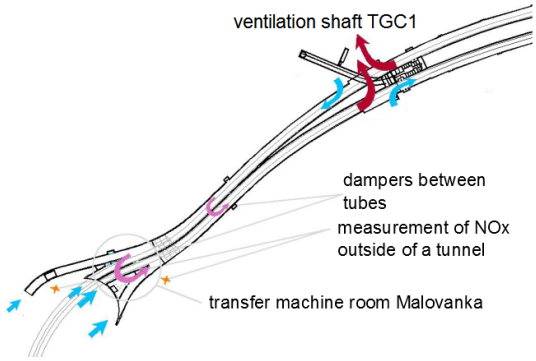

(b) Second level of protection.

Figure 5.4: Schematic situation of the first and second level of protection, respectively. Direction is denoted by arrows.[15]

of fresh air in the tunnel and dilute the polluted air, and thus satisfy given IAQ in the tunnel. This state is deactivated when the values of concentration of pollutant concentrations decreases bellow 75 % of the limit values. Possibly frequent switching between on and off mode in this state of operation is avoided by used hysteresis type of control. The automatic control should keep the values of pollutant concentrations in allowed range. The range is defined about 10 % more than limit values of given concentrations.

State 3: First level of protection

The State 3 is activated according to the traffic intensity as shown in Figure 5.3 and Table 5.2. The objective of this state is to maintain amount of air, which is exhausted from the northern tunnel to Malovanka area, under defined limit. The goal state is depicted in Figure 5.4a. The requirement is to keep the airflow in aerodynamic section 13, see FigureA.1, lower than 200 $m^3 s^{-1}$. The airflow is decelerated mainly by the ventilation room Střešovice and jet fans in the corresponding section.

Minimization of exhausted gases from the exit portal at Malovanka is the most complex task from the operational ventilation point of view. Furthermore, within the State 3 there are no additional requirements on the protection of other exit ramps in the Blanka tunnel complex, despite the Malovanka exit portal.

State 4: Second level of protection

The State 4 is able to avoid extraction of polluted air from tunnel ramps U Vorliku, Prašný most and mainly Malovanka, however it is more energy demanding that the first level of protection. The ideal state of this Second level of protection is expressed in Figure 5.4b.

The State 4 is activated based on the traffic intensity. Moreover, it is also switched on according to the outside air velocity at the portal Malovanka, see Table 5.2. This state is activated as soon as the airflow velocity decreases bellow 0.5 $\mathrm{m\,s^{-1}}$, since sufficient dispersion conditions for NO_x are not ensured if the airflow velocity is less than 0.5 $\mathrm{m\,s^{-1}}$ in the surrounding area of Malovanka portal.

The fresh air is provided through both tunnel ramps likewise VMR and the polluted air is exhausted from the tunnel through ventilation machine rooms. Particularly, there are dampers between the northern and souther tunnel tube on two places and also there is the machine room Malovanka. The polluted air from the northern tunnel is moved to the southern tunnel thanks to these dampers and the VMR Malovanka keeping the exit portal Malovanka in lower pressure compared to the surroundings of the tunnel portal. In addition, a minor part of the polluted air can be exhausted from the tunnel through Troja exit ramps, because there are no strict demands on ambient environment, since Troja ramps are situated outside build up area. Therefore, it is allowed to transfer air through these ramps.

In other words, the State 4 ensures airflow in entrance ramps to be positive and airflow in exit ramps to be negative. Compared to the State 3, the State 4 ensures requirements on ambient environment of all mentioned exit ramps, not only of the exit ramp at Malovanka.

State 5: Pre-ventilation

The pre-ventilation state is switched on if there is a suspicion of fire in tunnel sections. Special requirements on the longitudinal airflow velocity in a section are desired, if the fire pre-alarm is detected. In such case, the longitudinal airflow velocity should not decreased below 1.2 $\mathrm{m\,s^{-1}}$ in the tunnel section. The limit value of airflow velocity in case of fire, i.e. 1.2 $\mathrm{m\,s^{-1}}$, is critical for the transmission of smoke during evacuation phase in the fire-affected tunnel section.

5.4 Formulation of the optimization task

The optimization part is the core of the ventilation control system. This block assembles and solve the optimization task. The aim of the controller is such that the optimal control input is calculated based on several input parameters to fulfill al constraints, while minimizing electricity consumption. The currently used controller in the Blanka tunnel complex, depicted in Figure 5.5, is composed of a feed-forward and a feed-back part. Resulting control inputs are mostly influenced by the feed-forward part of the controller, thus the feed-forward part is only taken into account within this thesis.

5.4.1 Feed-forward part

The currently used controller uses the simplified steady-state model of airflow velocity described in Section 3, because the expression of a dynamic mathematical model of airflow velocity for complex road tunnels is difficult and a controller using this model would be computational time demanding.

The optimization task is assembled based on the tunnel data including NO_x, traffic data, opacity, fan data and according to the current state of the operational ventilation provided by the state switch described in Section 5.3.1. In this case, the cost function is given by the electric power of all ventilation devices including both jet fans and VMRs. Additionally, constraints are represented by the mathematical model of airflow velocity, required airflow velocities (soft constraints) and physical limitations of ventilation devices (hard constraints).

The control approach is based on the non-linear mathematical optimization, where the objective of the optimization task is to determine a minimum of a cost function. The optimization task can be state in the following way [33]

$$\begin{aligned} x^* &= \arg\min f_0(x) \\ &\text{subject to:} \\ f_i(x) &\leq 0, \quad i = 1, 2, ..., r \\ h_i(x) &= 0, \quad i = 1, 2, ..., s \end{aligned} \tag{5.1}$$

where x is the real number vector of decision variables, x^* is the optimal or suboptimal solution of the optimization task (5.1), $f_0(x)$ is the cost function, $f_i(x)$ represents inequality constraints, $h_i(x)$ denotes equality constraints and s, r is the total number of inequality and equality constraints, respectively.

The optimization task is calculated in 15 min intervals, i.e. the sampling time of the optimization task is 15 min. Actually, the feed-forward part of the high level controller is represented by the optimization task, since no information about measured airflow velocity is incorporated into the optimization.

5.4.2 Decision variables

The vector of decision variables is composed of airflow velocities, number of jet fans which are to be run, the desired airflows in VMRs and so-called slack variables ensuring the desired airflow velocities in individual section of the tunnel. The vector of decision variables can be written down for the tunnel ventilation control problem in the following

way

$$x = \left[v_1, ..., v_{v_n}, n_1, ..., n_{f_n}, Q_1, ..., Q_{v_{q_n}}, s_1, ..., s_{v_n}\right] \tag{5.2}$$

where $v_1, ..., v_{v_n}$ are the airflow velocities in respective sections of the tunnel, $n_1, ..., n_{f_n}$ denotes the number of jet fans, which are to be run in the corresponding group $JF_1, ..., JF_{f_n}$, $Q_1, ..., Q_{v_{q_n}}$ represents the desired airflow in the given VMR and $s_1, ..., s_{v_n}$ are the slack variables belonging to the individual desired airflow velocities in corresponding sections of the tunnel.

Adding slack variable s_i within the optimization task is a common practice to ensure feasibility. A slack variable relaxes a hard constraint for airflow velocity v_i to stay within allowable bounds $v_i \in (v_{\min}, v_{\max})$.[34]

Variables $n_1, ..., n_{f_n}$ and $Q_1, ..., Q_{v_{q_n}}$ give the resulting control input. These variables are hardly constrained, meaning that, there are a maximum number of jet fans to be possibly run and maximum volumetric flow rate of respective ventilation machine rooms. These hard constraints can be expressed as inequality constraints. In addition, number of jet fans $n_1, ..., n_{f_n}$, which are to be run, can posses positive or negative real values. The positive sign stands for the star-up of jet fans in the driving direction, and on the other hand, the negative sign means the start-up of jet fans against the driving direction.

$v_{v_n} = 37$ is the number of aerodynamic sections and airflow velocities, f_n is the number of groups with jet fans and $q_n = 11$ is the number of VMRs, thus there are 114 decision variables in total within the optimization tasks (5.1). Figure A.1 depicts division of the Blanka tunnel complex into aerodynamic sections.

5.4.3 Cost function

The cost function f_0 in the optimization task 5.1 represents summarized electric power of all ventilation devices, particularly, jet fans and ventilation machine rooms, and penalties when exceeding the desired range of airflow velocities

$$f_0(x) = \sum_{t=1}^{f_n} P_{f,i} + \sum_{i=1}^{q_n} P_{q,i} + \sum_{i=1}^{v_n} a_i \left(v_i - s_i\right)^2 \tag{5.3}$$

where $P_{f,i}$ is the power of the i-th group with jet fans, $P_{q,i}$ denotes the electricity power of the i-th ventilation machine room, v_i is a longitudinal airflow velocity in the i-th section and s_i represents a slack variable corresponding to the airflow velocity in the i-th section. Moreover, $v_i - s_i$ defines a variance of the airflow velocity from the desired range in the i-th section and a_i is a weight of penalty when exceeding the desired zone of airflow velocity.

Jet fan power

According to the [35] the formula of the jet fan power P_f can be expressed as follows

$$P_f = P_{\text{ref}} \cdot \omega_{\text{R}}^3 \tag{5.4}$$

where P_j is the actual power of jet fan, P_{ref} is the nominal power of a jet fan and ω_{R} denotes the relative speed of a jet fan, i.e. from 0 % to 100 % of nominal speed.

However the general formula (5.4) for the JF power is introduced, simplified relationship is used to calculate the total power od jet fans in the ith group [15]

$$P_{f,i} = P_{\text{ref},i} \cdot n_i \tag{5.5}$$

where n_i is the number of jet fans which are to be run in the ith group, i.e. the decision variable from the optimization task (5.1), n_i is a real number, which is splitted between jet fans with soft-starters and a jet fan with variable speed drive. [8]

The simplified formula (5.5) is used, because the relationship (5.4) is not suitable for the optimization task (5.1), since there is a cubic dependence of the jet fan power on the relative speed complicating the feasibility of the optimization task. Moreover, in almost each fan group together with jet fans with soft-starters, there is one jet fan with a variable speed drive enabling continuous speed regulation. Therefore, the decision variables are required to be split into two groups (jet fans wit variable speed drive and jet fans with soft-starters).

Power of ventilation machine rooms

The airflows in VMR are desired, because they are one of the decision variables in the optimization task (5.1), thus a relationship of fan power and airflow is requested.

There is a cubic relationship of the fan power P_f on the airflow Q_f [35]

$$P_f = P_{\text{ref}} \left(\frac{Q_f}{Q_{\text{ref}}} \right)^3 \tag{5.6}$$

where Q_f is the airflow of an axial fan in a VMR, P_{ref} is the nominal power of an axial fan and Q_{ref} is the nominal airflow of an axial fan in a VMR running at full speed.

A ventilation machine room is equipped with several axial jet fans. The relationship (5.6) is valid if all axial jet fans have the same parameters, such as jet fan diameter, nominal power and volumetric airflow rate. In addition, the characteristic (5.6) supposes the parallel operation of all jet fans during the real operation.

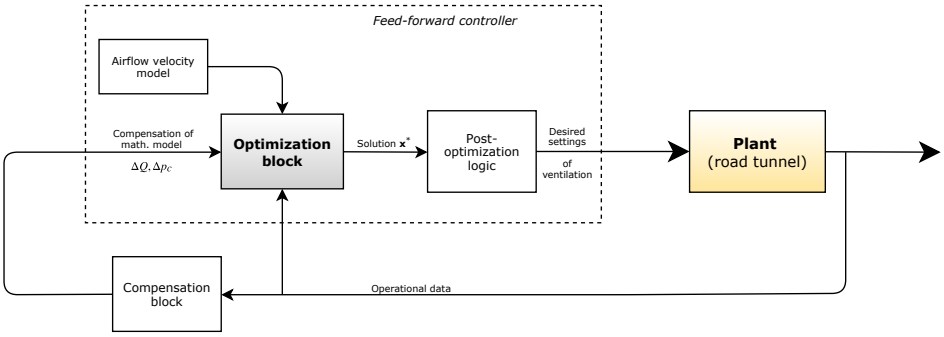

Figure 5.5: A currently used control structure of the operational ventilation in the Blanka tunnel complex. It is formed by the feed-forward part and adaptive logic.

5.4.4 Optimization task constraints

The optimization task (5.1) is a constrained minimization problem. There are two type of constrains, equality $h_i(x)$ and inequality $f_i(x)$ constraints, respectively. Equality constraints are represented by the mathematical model of airflow dynamics. In this case, the equality constraints are non-linear, because the first Kirchhoff's law denotes linear equality compared to the second Kirchhoff's law, which brings non-linear equality constraints, therefore the equality constraints $h_i(x)$ in the optimization task (5.1) depend non-linearly on airflow velocities in respective tunnel sections. Additionally, inequality constraints are given by hard-constraints, i.e. physical limitations of jet fans and VMRs, and soft-constraints denoting required airflow velocities.

Desired airflow velocities are achieved using soft-constraints enhancing the feasibility of the optimization task (5.1). There are strict demands on slack variables s_i rather on decision variables $v_1, ..., v_{v_n}$, while minimizing corresponding term $\sum_{i=1}^{v_n} a_i \left(v_i - s_i\right)^2$ in the cost function f_0 (5.3), because there are usually requirements to keep the airflow velocity in a tunnel section in desired bounds. The aforementioned term is composed of the slack variables s_i corresponding to airflow velocities in individual sections of the tunnel and a_i representing weighting coefficient. Moreover, it penalizes the violation of the desired bounds of airflow velocity, where the desired bound is defined by the slack variables s_i. The coefficient a_i sets a size of penalty, when exceeding the desired bounds of airflow velocity.

5.4.5 Feedback part

The feedback part of the high level controller is represented by the compensation block depicted in Figure 5.5. Deviations between the real measured data and the mathematical model of process dynamics are compensated based on minimizing differences in continuity equation and modification of pressure changes in Bernoulli equations. Detailed description

of the feedback part of the controller is provided in [8].

5.4.6 Solution of the optimization task

Several problems raise within the described optimization problem. It is a non-linear optimization problem, since the power of ventilation machine rooms depends non-linearly on the volumetric airflow rate, as denoted in Eq. (5.6), constraints given by the set of Kirchhoff's equations are non-linear and relationships describing pollutant concentration are hyperbolic in shape (Eqs. (4.19) and (4.20)).

Further, the optimization problem (5.1) is non-convex because the equality constraints given by the mathematical model of airflow dynamics are not affine, i.e. the generalized Bernoulli equation depends nonlinearly on airflow velocity v. According to [36], the so-called Sequential quadratic programming (SQP) method can be used to find solution of such optimization task like the introduced optimization problem (5.1) is. Detailed insight into the algorithm is provided in [36] as well. Unfortunately, there is no guarantee that the global optimum corresponding to the lowest possible value of cost function $f_0(x)$ (5.3) is found, because the optimization task (5.1) is non-convex. The computational environment MATLAB [4] is used to solve described optimization task, particularly, the function *fmincon* within the *Optimization toolbox* is used.

5.5 Finding a global solution

The main objective of the operational ventilation control is to ensure both IAQ and a protection on ambient environment at surroundings of given exit portal of the tunnel complex. Nevertheless the energy savings are not considered as the main goal, it is convenient to achieve significant reduction in electricity consumption, because operational ventilation forms important amount of energy costs of the tunnel operation. Thus finding the global solution of the optimization problem (5.1) is currently being relevant subject of an intensive research. There are several algorithms to determine a global minimum of non-convex optimization tasks.[8]

According to [37], moment relaxation algorithms can be applied in order to find the global solution, since the optimization task (5.1) is a polynomial problem. The moment relaxation algorithm unfortunately can not determine the global solution of complex and large-scale tasks. As it is known, the optimization problem (5.1) has 114 decision variables and many constraints including several quadratic equality constraints and the demands on the computational capacity are very high, therefore the moment relaxation algorithm is unable to use for solving the optimization problem (5.1) in real-time.

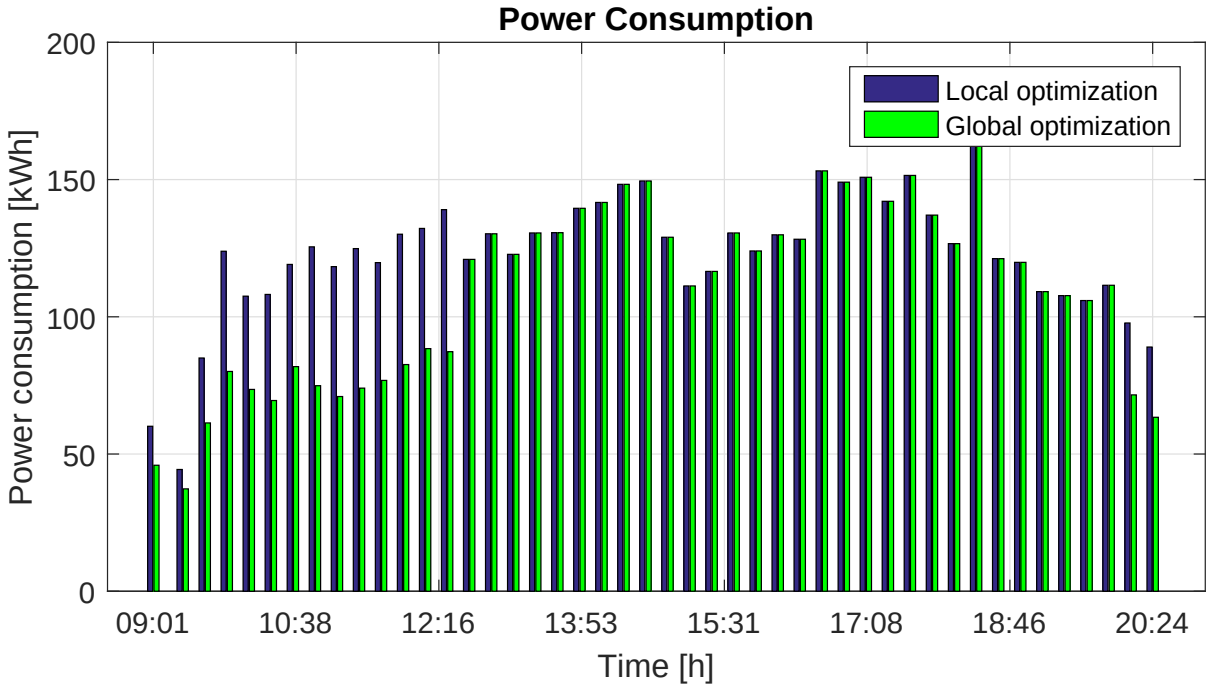

Figure 5.6: A comparison of electricity consumption within simulation day 1.

Other possible approach how to find the global solution of the optimization problem (5.1) is the branch and bounds algorithm based on linear programming relaxations and envelope approximations.[38] The branch and bound approach is based on the principle that the total set of feasible solutions can be evaluated systematically until the best solution is found. It also uses a tree diagram of nodes and branches to organize the solution partitioning. [39]. Moreover, the branch and bounds method computes better and better outer approximations and these are used to determine lower bounds of an optimization problem. However, the upper bounds are also calculated, they are used to prune the branch and bounds search tree. Therefore, the lower and upper bound solver needs to be appropriately set up before the algorithm starts.[8]

5.5.1 Simulation results

In this section the efficiency and contribution of the applied branch and bounds (B&B) algorithm solving the given optimization problem (5.1) is analyzed. The branch and bound approach solving the global optimization problem is also compared against the currently used SQP algorithm for the local optimization. Unfortunately, the comparison is not performed in real operation in the Blanka tunnel, nevertheless, computer simulations are provided and analyzed. The B&B algorithm might be implemented in the real operation in case of significant benefit in terms of power savings.

Unfortunately, the B&B algorithm is often slow (exponential worst case performance) [40], in this case the B&B algorithm calculates the global solution of the optimization task (5.1)

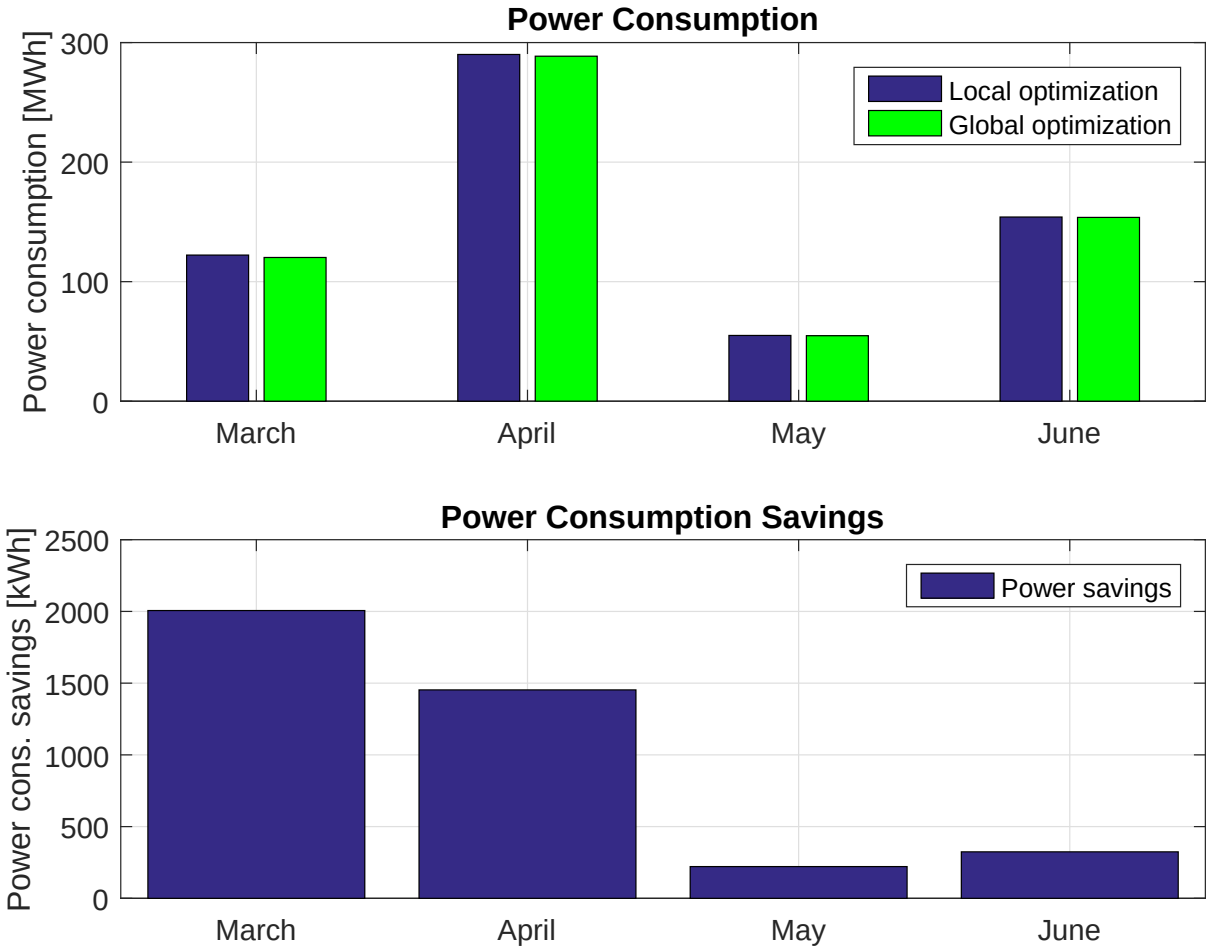

Figure 5.7: Evaluation of power consumption during simulation period.

in a reasonable time, yet the solution is still sensitive to choice of the lower and upper bound solver. For the computational purposes, a MATLAB based modeling language called YALMIP [41] is used. It can be used to model and solve optimization problems typically occurring in systems and control theory. Moreover, the YALMIP toolbox makes development of optimization problems uncomplicated. Rapid prototyping aiming to compose the optimization task (5.1) can be done using standard MATLAB commands.[42]. There are three different optimization problems during the branching. Upper bounds using a local nonlinear solver as well as lower bounds with defined solver and bound tightening using a linear programming solver. Within the simulations, the lower bound solver *fmincon* is chosen and the upper bound solver *fmincon* is set up. The *linprog* is chosen for bound tightening.

In depicted Figures 5.6, 5.7 and **??** the comparison of power consumption between the two approaches of finding the solution of the optimization problem (See Section 5.4), i.e. local and global optimization method, respectively, is shown. The control system calculates the optimum setting of ventilation devices every 15 min, allowing to consider the constant electric power within each 15 min period. This fact can be observed in

Month	**Energy savings** [kWh]
March	2006.1
April	1453
May	221.3
June	324.2
Sum	3944

Table 5.3: Power saving during simulation months.

Figure 5.6, where the average power consumption in a 15 min period is displayed within one simulation day. As evidenced, compared quantities differs from 9:00 AM to 0:15 PM and at the fall of the simulation day. Within these periods, proposed algorithm for finding global solution of (5.1) provides better solution (optimal solution), and thus energy costs are decreased. Moreover, based on this fact it is confirmed that the optimization algorithm within the currently used controller in the Blanka tunnel complex does not ensure the global minimum. Furthermore, during the rest of the simulation day both methods find the global minimum, hence resulting values of power consumption equal. The aforementioned behavior repeats among simulation days, as confirmed in Figure **??** and Figure 5.9. Data from the November 21st. to 24th. are evaluated in order to examine deeper the power consumption during a day. All simulations during given days are performed between 6:00 AM and 9:00 PM period.

In Figure 5.7, power consumption from March to June 2016 is compared. Electric consumption is shown in the upper graph, while the power consumption savings in the bottom graph. The blue columns presents resulting values of power consumption provided by the SQP method and the green columns denote resulting value given by the branch and bounds algorithm, in the first graph. On the other hand, power consumption savings for corresponding months are shown in the second graph. All quantities express the average daily values between 6:00 AM and 9:00 PM time section.

Based on aforementioned observations, power costs reduction is confirmed, when the global optimization method (B&B), which is capable of finding the global optimum of non-convex task, is applied. It is also proved that the Sequential quadratic programming algorithm does not ensure finding the global minimum, in many occasions it provides sub-optimal solution instead. In addition, however the global optimization method does not require to set up initial conditions for the solution finding procedure, compared to the local optimization method, it still provides valid solution in a reasonable computational time. As visible in Figure 5.7 simulation horizon is four months. Power savings in each month are shown in Table 5.3. During this period the power consumption is decreased approximately by 4 MWh in total. Hence, the energy savings can reach 12 MWh per

year, if it is assumed that total annual power consumption is directly proportional to the total consumption during the simulation horizon.

Therefore, applying the proposed branch and bound method in order to find the global optimum of the non-convex optimization task (5.1) successfully determines the optimal solution. And thus, global optimization approach may lead to decrease considerable amount of energy consumption of ventilation devices.

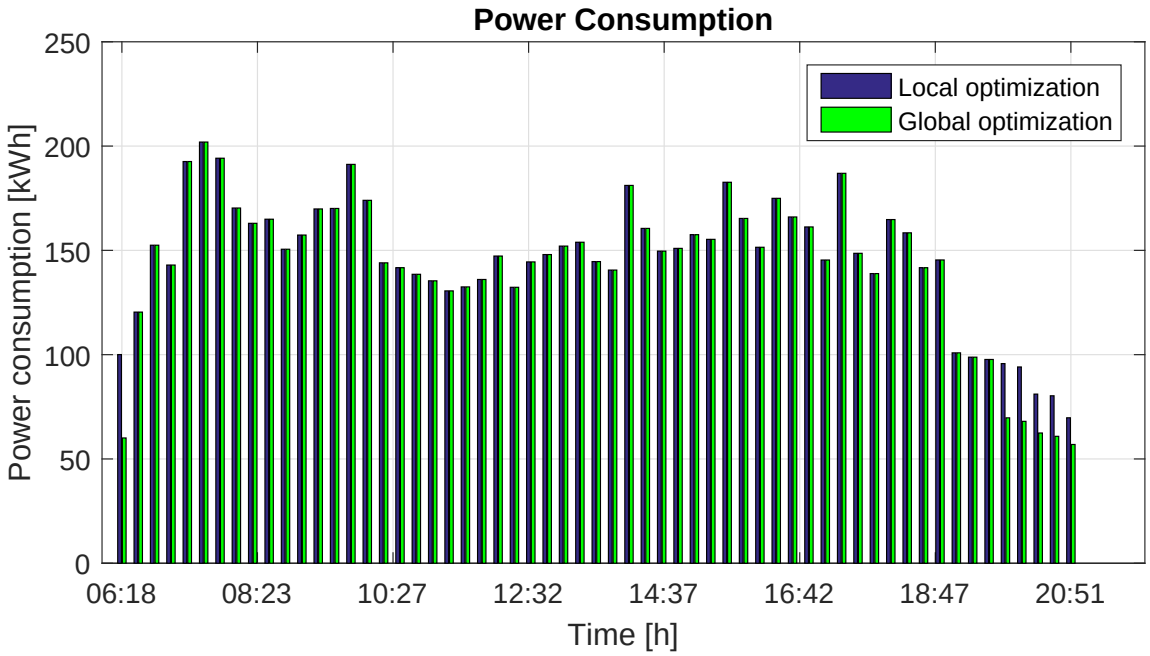

Figure 5.8: Power consumption comparison along simulation day 3.

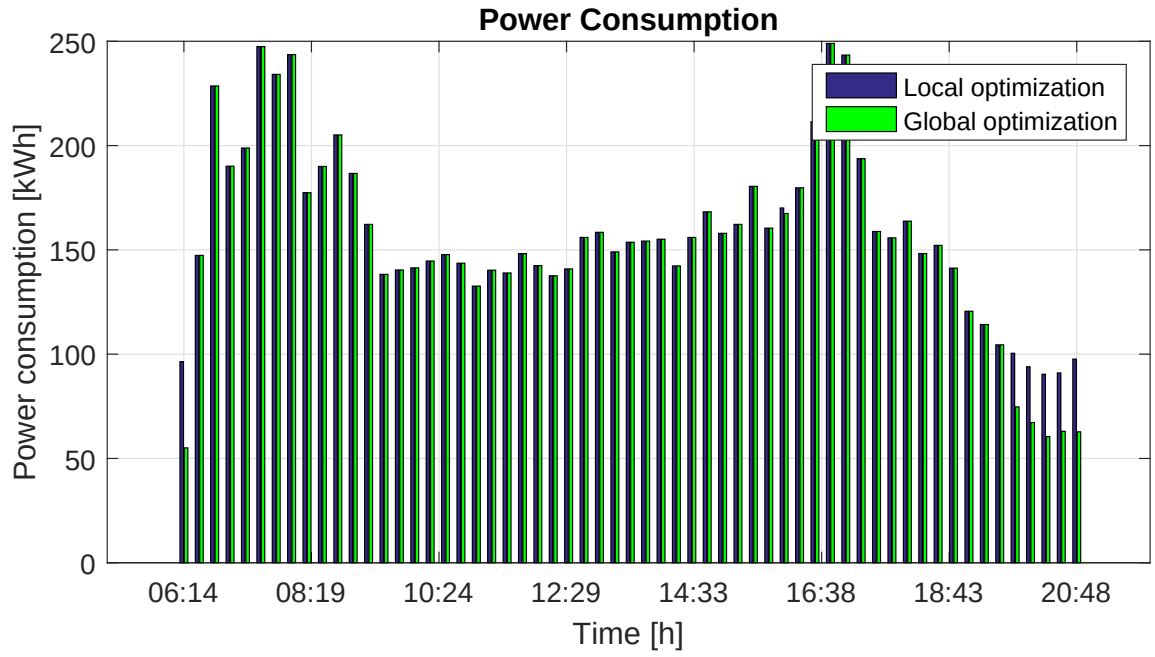

Figure 5.9: Power consumption comparison during simulation day 5.

6. Conclusion

This thesis contributes to problems of operational ventilation in the case study Blanka tunnel complex having complex structure and ventilation system.

The first goal of the thesis was to implement the steady-state linearized model of airflow velocity in the Blanka tunnel complex. The linearized model can be further used for the design of the operational ventilation control, especially, in the optimization procedure. Once the linearized model of process dynamics is found, quadratic programming can be used to solve an optimization task contributing significantly to the operational ventilation control design, because quadratic programming approach ensures finding the global optimum compared to the currently used controller in the Blanka tunnel complex.

The second goal of the thesis was to implement the dynamic model and also the steady-state model of pollutant concentrations. Section 4.4 provides comparison of both models with measured data from Blanka tunnel complex. Although there are certain level of inaccuracy between presented models and real data, denoted by Table 4.1, given models provide values of pollutant concentrations in allowable limits. The results from both models are satisfactory and they may lead to better performance of the controller in terms of estimating values of given concentrations. The aforementioned deviations are likely to be caused by ambiguous traffic information and distribution of passing cars within EURO categories as well as due to choice of initial conditions of the dynamic model.

The last main goal deals with finding the suitable method for solving the optimization task via global solution method. In Section 5.5.1, presented branch and bounds method is validated and resulting power consumptions are compared with values of energy consumption provided by the currently used controller in the Blanka tunnel complex based on the SQP approach. The results confirm usability of proposed B&B algorithm and they also stress out that electricity consumption of ventilation devices is reduced by using proposed branch and bounds algorithm while keeping the controller performance.

The aforementioned objectives of the thesis were fulfilled and achieved results can be applied on the Blanka tunnel complex in order to improve control performance and decrease electricity consumption.

A. **Appendix A**

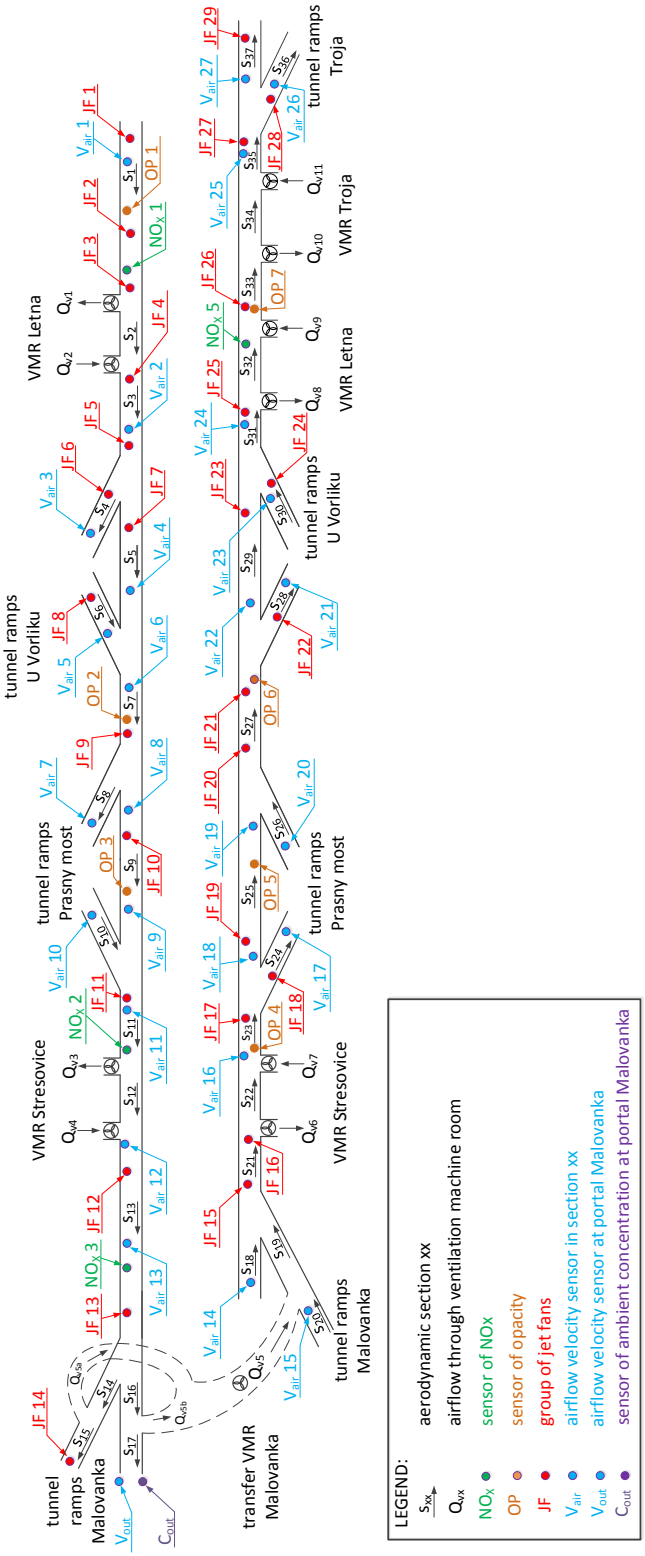

Figure A.1: A schematic illustration of the case study Blanka tunnel complex divided into aerodynamic sections. Position of measurement devices is shown as well as the position of jet fans and ventilation machine rooms.

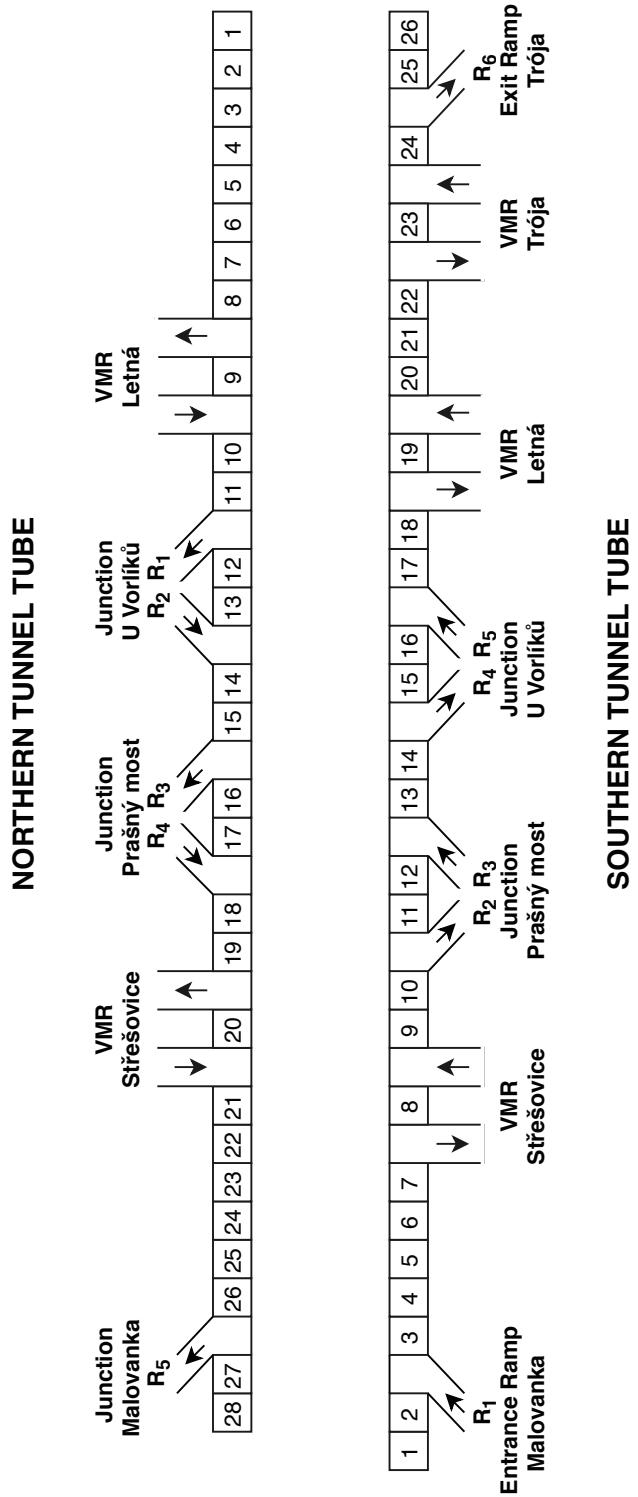

Figure A.2: A schematic illustration of the Blanka tunnel complex divided into sections including entrance and exit ramps. Location of ventilation machine rooms (VMR) is depicted. Requested airflow velocity direction is denoted by arrows, otherwise it corresponds to the direction of passing vehicles.

Bibliography

[1] Reliance; Industrial SCADA/HMI system, *Visualization of the tunnel traffic*. [Online]. Available: https://www.reliance-scada.com/Content/images/success-stories/transportation/tunel-valik/vizualizace_dopravy_large.jpg.

[2] SKANSKA, *Tunnel entrance of the elizabeth river tunnel*, 2013. [Online]. Available: http://blog.usa.skanska.com/wp-content/uploads/2013/06/9-Midtown-Tunnel1.jpg.

[3] H. Achour, J. Carton, and A. Olabi, "Estimating vehicle emissions from road transport, case study: Dublin city", *Applied Energy*, vol. 88, no. 5, pp. 1957 –1964, 2011, ISSN: 0306-2619. DOI: https://doi.org/10.1016/j.apenergy.2010.12.032. [Online]. Available: http://www.sciencedirect.com/science/article/pii/S0306261910005520.

[4] MATLAB, *Matlab 2015b*, https://www.mathworks.com/, 2015.

[5] I. E. Antelo, S. F. Martín, I. del Rey Llorente, and E. A. Álvarez, "Experiences on the specification of algorithms for fire and smoke control in road tunnels", in *New developments in tunnel safety : 5th International Conference Tunnel Safety and Ventilation*, Graz, Austria: Graz University of Technology, 2010. [Online]. Available: http://oa.upm.es/20941/.

[6] P. Pospisil and R. Brandt, "Smoke control in road tunnels.", pp. 1–6, May 2005.

[7] N. Euler-Rolle, M. Fuhrmann, M. Reinwald, and S. Jakubek, "Longitudinal tunnel ventilation control. part 1: Modelling and dynamic feedforward control", *Control Engineering Practice*, vol. 63, pp. 91 –103, 2017, ISSN: 0967-0661. DOI: https://doi.org/10.1016/j.conengprac.2017.03.017. [Online]. Available: http://www.sciencedirect.com/science/article/pii/S0967066117300758.

[8] J. Šulc, L. Ferkl, J. Cigler, and J. Pořízek, "Optimization-based control of ventilation in a road tunnel complex", vol. 69, pp. 141–155, Dec. 2017.

[9] D. Dimitris and R. William, *High-Resolution Methods for Incompressible and Low-Speed Flow*. Springer, Berlin, Heidelberg, 2005, ISBN: 978-3-540-26454-5. DOI: https://doi.org/10.1007/b137615.

[10] P. Swamee and A. K. Jain, "Explicit eqations for pipe-flow problems", vol. 102, pp. 657–664, May 1976.

[11] V. Talíř, "Identification of Models of Physical Processes in Road Tunnels", Master's thesis, Czech Technical University in Prague, 2015.

[12] William H. Frost, "Minor loss coefficients for storm drain modeling with swmm", *Journal of Water Management Modeling*, pp. 517 –546, 2006, ISSN: 2292-6062. DOI: https://doi.org/10.14796/JWMM.R225-23.

[13] H. Oertel, *Prandtl's Essentials of Fluid Mechanics*. Springer, New York, NY, 2004, ISBN: 978-0-387-21803-8. DOI: https://doi.org/10.1007/b97538.

[14] B. B. Daly, *Practical Guide to Fan Engineering*.

[15] Satra, spol s r.o., Data archives of the company.

[16] Ježek J., Váradiová B. and Adamec J., *Mechanika tekutin (in Czech)*. Prague: Czech Technical University in Prague, 2000.

[17] P. K.S. K. Sharma, *Design of Water Supply Pipe Networks*. John Wiley and Sons, Inc., 2008, ISBN: 9780470225059. DOI: 10.1002/9780470225059.

[18] R. Bellasio, "Modelling traffic air pollution in road tunnels", *Atmospheric Environment*, vol. 31, no. 10, pp. 1539 –1551, 1997, ISSN: 1352-2310. DOI: https://doi.org/10.1016/S1352-2310(96)00296-8. [Online]. Available: http://www.sciencedirect.com/science/article/pii/S1352231096002968.

[19] C. A. Colberg, B. Tona, W. A. Stahel, M. Meier, and J. Staehelin, "Comparison of a road traffic emission model (hbefa) with emissions derived from measurements in the gubrist road tunnel, switzerland", *Atmospheric Environment*, vol. 39, no. 26, pp. 4703 –4714, 2005, ISSN: 1352-2310. DOI: https://doi.org/10.1016/j.atmosenv.2005.04.020. [Online]. Available: http://www.sciencedirect.com/science/article/pii/S1352231005003717.

[20] J. Šulc, "Ventilation control of the blanka tunnel", Master's thesis, Czech Technical University in Prague, 2012.

[21] World Road Association (PIARC), *Road tunnels manual*, 2011.

[22] Ohashi, H. er al., "Model-based airflow controller design for fire ventilation in road tunnels", *Proc. 4th International Symposium on the Aerodynamics and Ventilation of Vehicle Tunnels*, pp. 31–47, 1982.

[23] L. Kurka, L. Ferkl, O. Sládek, and J. Porízek, "Simulation of traffic, ventilation and exhaust in a complex road tunnel", *IFAC Proceedings Volumes*, vol. 38, no. 1, pp. 60 –65, 2005, 16th IFAC World Congress, ISSN: 1474-6670. DOI: https://doi.org/10.3182/20050703-6-CZ-1902.02033. [Online]. Available: http://www.sciencedirect.com/science/article/pii/S1474667016380454.

[24] Ferkl, L. and Sládek, O. and Pořízek, J., "Tunnel ventilation simulation of the city ring in prague", *Tunnelling and Udnerground Space Technology 21*, pp. 443–443, 2006.

[25] C. C. Lee, "Fuzzy logic in control systems: Fuzzy logic controller. i", *IEEE Transactions on Systems, Man, and Cybernetics*, vol. 20, no. 2, pp. 404–418, 1990, ISSN: 0018-9472. DOI: 10.1109/21.52551.

[26] Wikipedia contributors, *Wikipedia, the free encyclopedia*, 2018. [Online]. Available: https://www.wikipedia.org/.

[27] E. Karakaş, "The control of highway tunnel ventilation using fuzzy logic", *Engineering Applications of Artificial Intelligence*, vol. 16, no. 7, pp. 717 –721, 2003, ISSN: 0952-1976. DOI: https://doi.org/10.1016/S0952-1976(03)00068-X. [Online]. Available: http://www.sciencedirect.com/science/article/pii/S095219760300068X.

[28] S. Bogdan, B. Birgmajer, and Z. Kovačić, "Model predictive and fuzzy control of a road tunnel ventilation system", *Transportation Research Part C: Emerging Technologies*, vol. 16, no. 5, pp. 574 –592, 2008, ISSN: 0968-090X. DOI: https://doi.org/10.1016/j.trc.2007.11.004. [Online]. Available: http://www.sciencedirect.com/science/article/pii/S0968090X07000897.

[29] E. Camacho, C. Bordons, and C. Alba, *Model Predictive Control*, ser. Advanced Textbooks in Control and Signal Processing. Springer London, 2004, ISBN: 9781852336943. [Online]. Available: https://books.google.cz/books?id=Sc1H3f3E8CQC.

[30] J. Hrbček and V. Šimák, "Implementation of multi-dimensional model predictive control for critical process with stochastic behavior", in *Advanced Model Predictive Control*, T. Zheng, Ed., Rijeka: InTech, 2011, ch. 6. DOI: 10.5772/16364. [Online]. Available: https://doi.org/10.5772/16364.

[31] J. Hrbček, J. Spalek, and V. Šimák, "Process model and implementation the multivariable model predictive control to ventilation system", pp. 211 –214, Mar. 2010.

[32] CETU, *Dossier pilote des tunnels quipements. (4.1)*, November 2003.

[33] Stephen Boyd, *Course convex optimization; lecture slides*, Sumer Quarter 2013 - 2014. [Online]. Available: https://web.stanford.edu/class/ee364a/lectures.html.

[34] X. Chen, Q. Wang, and J. Srebric, "Occupant feedback based model predictive control for thermal comfort and energy optimization: A chamber experimental evaluation", *Applied Energy*, vol. 164, pp. 341 –351, 2016, ISSN: 0306-2619. DOI: https://doi.org/10.1016/j.apenergy.2015.11.065. [Online]. Available: http://www.sciencedirect.com/science/article/pii/S0306261915015159.

[35] A. Chatterjee, L. Zhang, and X. Xia, "Optimization of mine ventilation fan speeds according to ventilation on demand and time of use tariff", *Applied Energy*, vol. 146, pp. 65 –73, 2015, ISSN: 0306-2619. DOI: https://doi.org/10.1016/j.apenergy.2015.01.134. [Online]. Available: http://www.sciencedirect.com/science/article/pii/S0306261915001749.

[36] S. Boyd and L. Vandenberghe, *Convex Optimization*. New York, NY, USA: Cambridge University Press, 2004, ISBN: 0521833787.

[37] J.-B. Lasserre, "Global optimization with polynomials and the problem of moments", vol. 11, Sep. 2004.

[38] G. P. McCormick, "Computability of global solutions to factorable nonconvex programs: Part i — convex underestimating problems", *Mathematical Programming*, vol. 10, no. 1, pp. 147–175, 1976, ISSN: 1436-4646. DOI: 10.1007/BF01580665. [Online]. Available: https://doi.org/10.1007/BF01580665.

[39] B. Taylor, *Integer programming: The branch and bound method*. [Online]. Available: http://web.tecnico.ulisboa.pt/mcasquilho/compute/_linpro/TaylorB_module_c.pdf.

[40] Stanford University, *Lecture slides - EE364b: The Branch and Bound Method*. [Online]. Available: http://web.tecnico.ulisboa.pt/mcasquilho/compute/_linpro/TaylorB_module_c.pdf.

[41] J. Löfberg, "Yalmip : A toolbox for modeling and optimization in matlab", in *In Proceedings of the CACSD Conference*, Taipei, Taiwan, 2004.

[42] J. Lofberg, "Yalmip : A toolbox for modeling and optimization in matlab", in *2004 IEEE International Conference on Robotics and Automation (IEEE Cat. No.04CH37508)*, 2004, pp. 284–289. DOI: 10.1109/CACSD.2004.1393890.